# A Review of the Migration of Hydrogen from the Planetary to Basin Scale

**Bhavik Harish Lodhia, Luk Peeters, Emanuelle Frery**

[1]CSIRO Environment, Kensington, Perth, 6151, WA, Australia
[2]CSIRO Environment, Waite, Adelaide, 5064, SA, Australia
[3]CSIRO Energy, Kensington, Perth, 6151, WA, Australia

**Key Points:**

- History of planetary formation and overview of natural hydrogen cycle of Earth.
- Summary of mechanisms for hydrogen migration (diffusion and advection), generation and consumption by microbial reactions.
- Summary of indicative timescales of hydrogen migration within crystalline and sedimentary rocks.

Corresponding author: Bhavik Harish Lodhia, Bhavik.Lodhia@csiro.au

**Abstract**

The occurrence of natural hydrogen and its sources have been reviewed extensively in the literature over the last few years, with current research across both academia and industry focused on assessing the feasibility of utilising natural hydrogen as an energy resource. However, gaps remain in our understanding of the mechanisms responsible for the large-scale transport of hydrogen and migration through the deep and shallow Earth and within geological basins. Due to the unique chemical and physical properties of hydrogen, the timescales of migration within different areas of Earth vary from billions to thousands of years. Within the shallow Earth, diffusive and advective transport mechanisms are dependent on a wide range of parameters including geological structure, microbial activity, and subsurface environmental factors. Hydrogen migration through different media may occur from geological timescales to days and hours. We review the nature and timescale of hydrogen migration from the planetary to basin-scale, and within both the deep and shallow Earth. We explore the role of planetary accretion in setting the hydrogen budget of the lower mantle, discuss conceptual frameworks for primordial or deep mantle hydrogen migration to the Earth's surface and evaluate the literature on the lower mantle's potential role in setting the hydrogen budget of rocks delivered from the deep Earth. We also review the mechanisms and timescales of hydrogen within diffusive and advective, fossil versus generative and within biologically moderated systems within the shallow Earth. Finally, we summarise timescales of hydrogen migration through different regions within sedimentary basins.

## Plain Language Summary

Over the last several years, naturally-occurring hydrogen has emerged as a potential game changer in the energy transition. However, the vast majority of current research focuses on understanding hydrogen generation and underground storage. Important questions remain - how did hydrogen come to be within Earth? What are the timescales of hydrogen movement through different regions of Earth and within different rock types? In this review, we describe the processes responsible for entraining hydrogen into Earth's mantle during the time of planetary formation and timescale of evolution towards the present-day hydrogen cycle. We summarise the importance of environmental factors and mineralogy for hydrogen movement and the timescale of generative and destructive processes in the shallow Earth. Finally, we summarise the timescale of hydrogen movement within different regions of Earth from the planetary to basin-scale and within different minerals and rock types.

## 1 Introduction

Hydrogen is regarded as an important component of the world's transition towards a low emission, net-zero future (IEA, 2021). Significant efforts are currently being made across academia and industry to improve our understanding of hydrogen subsurface mobility, especially in the context of natural hydrogen occurrence and underground storage (e.g., Zgonnik (2020); Muhammed et al. (2022); L. Wang, Jin, et al. (2023)). Within the literature, the term 'natural hydrogen' describes the hydrogen which is not manufactured and is directly found in the subsurface. Natural Hydrogen is encountered as a free gas (i.e., surface seeps), dissolved in groundwater and within fluid inclusions in rocks. Natural hydrogen migrates through a wide range of mechanisms, including diffusion (e.g., through crystalline lattices) and advection (e.g., dissolution in groundwater, migration along faults) (e.g. Farver (2010); Lefeuvre et al. (2021, 2022); Strauch et al. (2023); Truche et al. (2024)). Whilst laboratory experiments and assessments of specific case studies have shed some light on the complex nature of natural hydrogen migration, large gaps remain in our understanding of the mechanisms responsible for the large-scale migration of hydrogen through the deep Earth and within sedimentary basins. In this review, we refer

to the regions beneath the lithosphere, i.e. mantle, as the 'deep' Earth, and subsurface regions within geological and sedimentary basins as the 'shallow' Earth.

This review overviews the processes responsible for setting Earth's hydrogen budget and the timescales of hydrogen migration across all length-scales within Earth. We review (i) the origin of primordial or deep mantle natural hydrogen supply to the deep Earth, the role of water on mantle mixing and Earth's hydrogen cycle over geological timescales and (ii) the dynamics of diffusive and advective hydrogen migration within the shallow Earth on geological to human timescales.

## 2 Hydrogen in the deep Earth

Hydrogen is unlike any other molecule. Whilst it is the most abundant element in the universe, molecular hydrogen is scarce on Earth. Estimates of the hydrogen abundance in Earth's interior have spanned a range from less than the equivalent of the current hydrosphere to on the order of 100 hydrospheres if hydrogen is the dominant light alloying component in Earth's outer core (Williams & Hemley, 2001). There is a limited understanding of its sources, migration through rocks and whether hydrogen can accumulate in geological formations for significant time periods. To understand the nature of hydrogen migration within Earth, we must first consider its origins and distribution on a planetary scale. Within the deep Earth, there exist reservoirs of primordial or deep mantle hydrogen trapped during the period of planetary formation, which are proposed by some models to be transported by advection within the mantle on timescales of billions of years (Peslier et al., 2017; Loewen et al., 2019). For a detailed description of the mineralogical composition and hydrogen content of the deep Earth, see Williams and Hemley (2001). Following planetary accretion, the stabilisation of liquid water on the surface and onset of plate tectonics had a profound impact on the dynamics of mantle flow and Earth's hydrogen cycle. This includes the contamination of non-native material into Earth's mantle at subduction zones and its heterogeneity in mantle hydrogen contents. Conversely, the preservation of isotopic signatures indicate that mantle material delivered to Earth's surface at hotspot settings preserve their deep mantle or primordial isotopic signatures and do not mix with surrounding mantle (Mangenot et al., 2023). The timescale of hydrogen transport from within the deep Earth to different geological settings at the surface vary across several orders of magnitude. In this section, we describe the discrepencies between hydrogen and helium isotopic ratios encountered in rocks from different geological settings and compare frameworks for hydrogen migration to the Earth's surface from the deep mantle.

### Global hydrogen cycle

Whilst up to 90% of the proto-solar nebula comprised of hydrogen, $^{1}$H, the isotopes deuterium, $^{2}$H, and Helium-3, $^{3}$He, were also created during the Big Bang. Unlike terrestrial $^{4}$He, which is mainly produced by decay of uranium and thorium, terrestrial $^{3}$He is largely of primordial origin, synthesised in the aftermath of the Big Bang (Bania et al., 2002) and incorporated into the Earth primarily during its formation (Lupton & Craig, 1975). In spite of its primordial status and 4.56 Ga of planetary evolution, up to $\sim 2$ kg $^{3}$He continues to leak from Earth's interior and mainly along mid ocean ridges (Olson & Sharp, 2022). The reference proto-solar $D/H$ ratio is $\sim 2.1 - 2.5 \times 10^{-5}$, which is close to the Big Bang value. Due to its mass, hydrogen is lost through diffusion preferentially over deuterium and the $D/H$ ratio increases with geologic time. As $^{4}$He is a decay product of U-Th-Pb $\alpha$-decay systems, $^{3}$He/$^{4}$He ratios with Earth decrease monotonically with time, with high $^{3}$He/$^{4}$He rocks indicating preservation in mantle domains that are not modified by convective mixing or diffusive homogenisation since early Earth history (Porcelli & Elliott, 2008; Huang et al., 2014; Cooke et al., 2014; Lis et al., 2019). The reaction of deuterium, hydrogen and water, HD + $H_2O \rightleftharpoons H_2$+ HDO, is an impor-

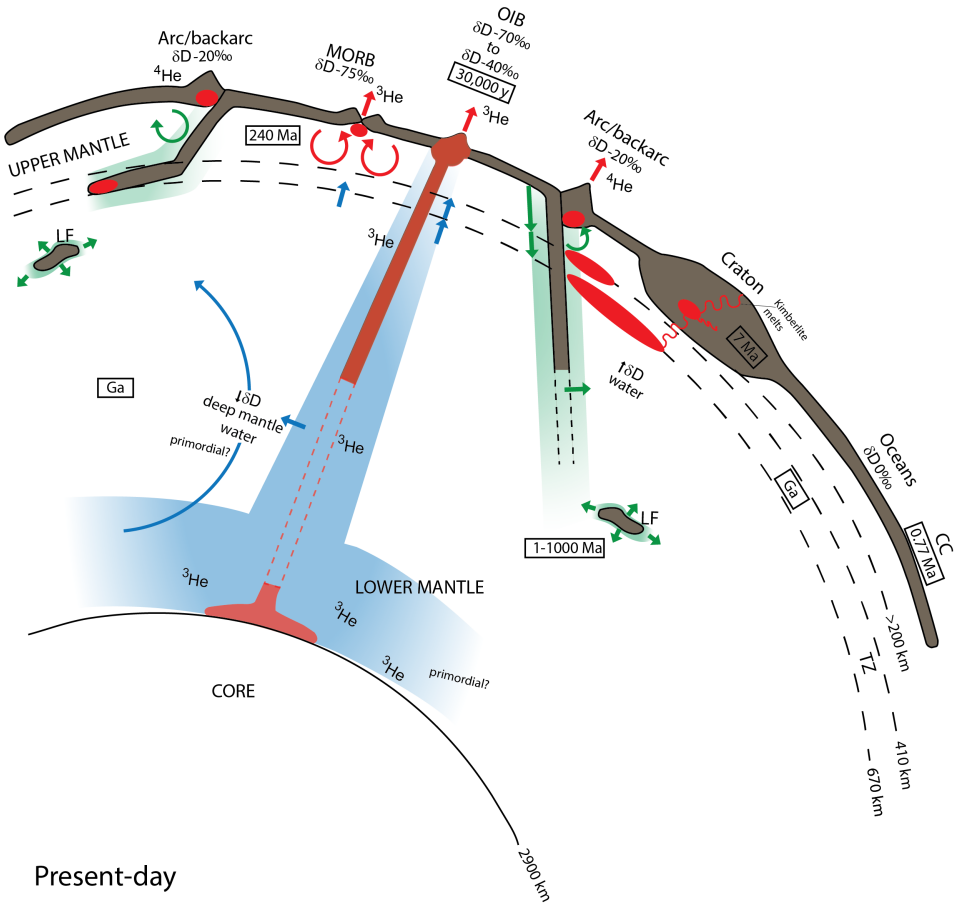


**Figure 1.** Conceptual model for primordial or deep mantle hydrogen and helium migration through Earth and present-day subduction patterns. Blue shading indicates regions of depleted mantle that sample reservoirs of primordial or deep mantle water, H and He. Green shading indicates infiltration of non-mantle water as a consequence of tectonic process on Earth's surface. Lithospheric fragments (LF) which break from subducting slabs may constitute a source of non-mantle material to the deep mantle (e.g. (Sperner et al., 2001; Zahirovic et al., 2016; van der Meer et al., 2018; Kufner et al., 2021)). The asthenosphere is a region within the upper mantle and beneath the lithosphere in which there is relatively low resistance to plastic deformation due to the partial melting of rocks initiated by the infiltration of hydrous mineral phases entrained on subducting lithosphere. The depth of the asthenosphere varies throughout Earth, however generally lies between 80 – 200 km depth. TZ = transition zone, red ovals = regions of partial melting in the upper mantle, lithosphere and TZ. Boxes = hypothesised residence times of water within different layers of Earth; Ga = billion years, Ma = million years (Bodnar et al., 2013). Continental and lithospheric thicknesses are not to scale. Modified from (Peslier et al., 2017; Loewen et al., 2019).

tant measure of the thermal history of water molecules since the formation of Earth. The $D/H$ ratio is expressed in delta notation as $\delta$D, whereby $\delta D = [(D/H)_{sample}/(D/H)_{V_{SMOW}} - 1]\times 10^3$ with $V_{SMOW}$ the Vienna Standard Mean Ocean Water. Hence, low $\delta$D values within high $^3$He/$^4$He rocks may be used as a diagnostic isotopic signature to determine the origins of water and mantle material within Earth (Geiss & Gloeckler, 1998; Loewen et al., 2019; Pinti, 2021).

Mid Ocean Ridges are transform margins where upwelling mantle is extruded at Earth's surface to form new oceanic crust. Mid-Ocean Ridge Basalts (MORBs) are mafic rocks derived from larger mantle domains that appear to sample deep mantle hydrogen transported to the melting domain in the upper mantle by large-scale mantle convection and typically have low $\delta$D values of $\sim -70$‰(Table 1) (Craig & Lupton, 1976; Rison & Craig, 1983; Poreda et al., 1986; Graham, 2002; Jackson et al., 2017; Loewen et al., 2019). $^3$He/$^4$He ratios in MORBs are typically homogeneous and have a narrow range of $7 - 9$ R$_A$, whereby R$_A$ = atmospheric ratio (C. J. Allègre et al., 1995; Gautheron & Moreira, 2002). Helium ratios analysed in MORB glasses by C. J. Allègre et al. (1995) from individual ridge segments show a linear correlation with the ridge spreading rate. Average helium ratios of MORBs are predominantly uniform and distinct from lower mantle and transition zone values, which is interpreted by C. J. Allègre et al. (1995) to indicate the existence of two scale upper mantle convection. Rapid convection within the uppermost mantle that feeds mid ocean ridges (see red arrows on Figure 1) is responsible for the homogenisation of helium in this layer and is calculated to have a mixing time of $\sim$ 250 Ma, which is distinct from the $\sim$ 1 Ga residence time of upper mantle rocks (C. Allègre et al., 1983; C. J. Allègre et al., 1995) (Figure 1).

Whilst enriched compared to non-mantle rocks, helium ratios in MORBs are significantly less than those found at Ocean Island Basalt (OIB) and Continental Hotspot (CH) settings, which can reach values $< 40$R$_A$ (Table 1). Although the nature of plume development over geological time remains an active topic of research, it is widely accepted that mantle plumes which feed OIB and CH settings may extend as deep as the core/mantle boundary ($\sim$ 2900 km) (Figure 1). Plumes that transport lower mantle rocks with high $^3$He/$^4$He and low $\delta$D signatures that are enriched in deep mantle water, i.e. water that has never been present at Earth's surface, are significant as they are conduits of deep mantle hydrogen and helium entrained in ultramafic rocks that are extruded at Earth's surface. Recent investigations into the architecture of hotspot-plume systems suggest that material transported via hotter and more buoyant mantle plumes have increased resilience to mixing with surrounding mantle and increased preservation of deep mantle geochemical signatures compared to colder and less buoyant plumes (Samuel & Farnetani, 2003; S. C. Lin & Keken, 2006; Garnero et al., 2016; Jackson et al., 2017; Jimenez-Rodriguez et al., 2023). It is noteworthy that CH setttings exhibit $\delta$D values close to MORB, however $^3$He/$^4$He ratios are significantly higher ($< 20$ R$_A$). Some, like the African hotspots, also have $\delta$D values as low as $-89$‰(Table 1) (Jimenez-Rodriguez et al., 2023). Furthermore, experimental results from Mangenot et al. (2023) indicate that $H_2$ is sensitive to isotope re-equilibration (e.g. between $H_2$ and water at its source) during the ascent and cooling of high-temperature crustal, magmatic, and mantle fluids. These observations indicate that material transport from the lower mantle must be fast enough to prevent mixing with both upper mantle and the surrounding continental cratonic rocks and significantly faster than the timescale upper mantle mixing. Hence, we hypothesise that the degree of enrichment of deep mantle hydrogen and helium within rocks delivered to OIB and CH settings, and therefore their surrounding terrestrial environments through subsurface processes e.g. serpentinisation, is controlled by the rate at which rocks are supplied from lower mantle reservoirs. This must be on the timescale of, at least, millions of years instead of hundreds of millions of years. Thus, the timescale of migration of rocks enriched in hydrogen from within the deep Earth varies over several orders of magnitude between different geological regimes and is distinct from water residence times.

Hence, it is likely that whilst the background flux of primordial or deep mantle hydrogen to upper mantle regions which supply melt to Mid Ocean Ridges is set by large-scale mantle convection over billions of years, the mixing of primordial or deep mantle hydrogen and helium-enriched material into the upper mantle is an order of magnitude faster over hundreds of millions of years.

178 **Primordial versus deep mantle hydrogen and helium ratios**

179 Although the primordial origins of $^3$He are generally accepted, there is controversy
180 within the scientific community regarding application of $^3$He/$^4$He ratios as a diagnos-
181 tic marker for primordial material. The value of the $^3$He/$^4$He ratio from the local inter-
182 stellar medium (LISM) is $1.7\pm0.8\times10^{-4}$, and is around two orders of magnitude greater
183 than the present-day atmospheric value, $R_A = 1.4\times10^{-6}$ (Graham (2002); Salerno et
184 al. (2003), see Table 1). LISM values are consistent with protosolar ratios obtained from
185 meteorites and Jupiter's atmosphere, supporting the hypothesis that negligible changes
186 of the abundance of $^3$He occurred in the galaxy during the past 4.5 Ga (Salerno et al.,
187 2003). High $^3$He/$^4$He ratios in Ocean Island Basalts (OIBs) were traditionally interpreted
188 as indicators of a primitive, undegassed mantle source that has been trapped within the
189 Earth to the present day (Bouhifd et al., 2013). This interpretation was predicated on
190 the assumption that these ratios reflect the composition of material sampled by rapidly
191 ascending thermally buoyant plumes arising from deep within the mantle (Kurz et al.,
192 1982; Morgan, 1971; Kellogg & Wasserburg, 1990). Despite this established view, pri-
193 mordial models fail to account for observed discrepancies in helium concentrations and
194 the elemental ratios of He and other noble gases (e.g. Ar and Ne) between OIBs and Mid-
195 Ocean Ridge Basalts (MORBs), with the former displaying values an order of magni-
196 tude lower than those found in MORBs (Gonnermann & Mukhopadhyay, 2007).

197 The debate over the origins of high $^3$He/$^4$He ratios in OIBs and how these ratios
198 address the helium paradoxes has been extensively explored in the literature. Gonnermann
199 and Mukhopadhyay (2007) present a model in which the helium concentration paradox,
200 as well as the variance in noble-gas concentrations observed in MORB and OIB glasses,
201 can be explained by disequilibrium open-system degassing of erupting magma. Their work
202 suggests that higher $CO_2$ content in OIBs leads to more extensive helium degassing in
203 OIB magmas compared to MORBs, thus deriving noble gases in OIB lavas from a largely
204 undegassed primitive mantle source. This interpretation aligns with the conventional view
205 that high $^3$He/$^4$H ratios in OIBs indicate parts of the deep mantle have remained iso-
206 lated from outgassing and the convective upper mantle over Earth's history (Gonnermann
207 & Mukhopadhyay, 2007).

208 Bouhifd et al. (2013) assess helium partitioning in experiments between molten sil-
209 icates and iron-rich metal liquids at conditions representative of Earth's lower mantle
210 and core. Their results and estimated concentrations of primordial helium suggest that
211 significant quantities of helium may reside in the core and that the early core could have
212 incorporated enough helium to supply deep-rooted plumes enriched in $^3$He throughout
213 Earth history. Bouhifd et al. (2013) therefore suggest that two variations in the $^3$He/$^4$He
214 ratio observed at the surface in OIBs and MORBs may be explained by two distinct reser-
215 voirs in the Earth's interior (e.g. Hopp and Trieloff (2008)). These are a conventional
216 depleted mantle source and a deep, still enigmatic, source that must have been isolated
217 from processing throughout Earth history. However, modelling of helium ingassing into
218 a silicate magma ocean and iron-rich proto-core coupled to a nebular atmosphere of so-
219 lar composition and outgassing into a coupled core-mantle system after accretion by Olson
220 and Sharp (2022) indicates that Earth's core may be a substantial and long-lived reser-
221 voir of primordial helium.

222 Zhu et al. (2020), however, offer a contrasting perspective by proposing that he-
223 lium contents and $^3$He/$^4$He isotopic ratios can be fractionated by thermal diffusion in
224 the lower mantle, driven by an adiabatic or convective temperature gradient. Their model
225 suggests that the lower mantle is helium stratified due to thermal diffusion, resulting from
226 a of $\sim$ 400 K temperature contrast across the lower mantle. Hence, Zhu et al. (2020)
227 argue that helium fractionation, rather than the lower mantle being a primordial and
228 undegassed reservoir, explains the observed high $^3$He/$^4$H isotopic ratios and lower he-
229 lium contents in OIBs. Zhu et al. (2020) argue that OIBs derived from the deepest lower
230 mantle, which display high $^3$He/$^4$H isotopic ratios and less helium content, can be ex-

plained by their model, effectively addressing the long-standing helium concentration paradox without necessitating a primordial undegassed lower mantle reservoir.

These differing viewpoints illustrate the complexity of mantle dynamics and the origins of helium isotopic variations and their implications for characterising truly primordial source material. It is beyond the scope of this review to explore this subject in greater detail, however it is widely accepted that isotopic signatures may be used to diagnose the preservation of deep lower mantle material over geologically significant time periods transported rapidly over planetary length scales (e.g., Mackintosh and Ballentine (2012)). However, whilst the influence of primordial material on rocks that preserve high $^3He/^4$/He isotopic signatures rocks are debated, we acknowledge that this cannot be excluded entirely.

## The impacts of water on the deep Earth and early tectonics

As isotopic signatures of igneous rocks may be used to identify material sourced from deep lower mantle reservoirs, they offer an insight into the hydrogen cycle of the deep Earth. Whilst the diffusion of water and hydrogen in silicates is fast compared to other elements, it cannot explain the heterogeneity of lower mantle material or enrichment within rocks delivered by mantle plumes or upwelling. In the absence of water infiltration into the deep mantle, mantle convection alone would lead to homogeneous water contents among regions of more than $\sim 100$ km size (Peslier et al., 2017). For typical asthenospheric conditions, diffusion of hydrogen over a distance of $\sim 10$ km takes $\sim 1$ Ga (Karato, 2007; Peslier & Bizimis, 2015; Peslier et al., 2017). Estimates of the residence time of water within different layers in Earth are calculated by Bodnar et al. (2013) as $< 3000$ years for the hydrosphere, $0.77 - 7$ Ma (million years) for the lithosphere and $\sim$ Ga (billion years) for the transition zone and lower mantle (Figure 1).

Combined evidence from several radionuclide systems (Pd-Ag, Mn-Cr, Rb-Sr, U-Pb) suggests that water was not incorporated in Earth in significant quantities until the planet had grown to $\sim 60 - 90\%$ of its current size, while core formation was still ongoing (Peslier et al., 2017). Prior to the onset of plate tectonics, some models propose that the early Earth lost heat generated from planetary accretion and radioactive decay of isotopes in the metallic core through degassing and volcanism according to a stagnant or mobile lid regime during the late Hadean (Solomatov & Moresi, 2000; Capitanio et al., 2022). The fractionation of Earth into the core, mantle and early crust is proposed by those models to have created a stratified water structure within the planet. During this period, photolysis from solar radiation and late crust-forming events led to significant loss of water from the early crust and upper mantle, leading to the lower mantle becoming relatively enriched in primordial or lower mantle water, hydrogen and helium (Peslier et al., 2017). The gradual accumulation of liquid water oceans is generally accepted to be a result of the impact of chondritic material from the asteroid belt following the period of heavy bombardment and stabilisation of Earth's late veneer. Depending on which estimates are used for the water and carbon contents of the bulk silicate Earth, $20 - 100\%$ of the early mantle's hydrogen and carbon may have been brought to Earth by carbonaceous chondrites during this late stage of planetary formation (Marty & Yokochi, 2006; Z. Wang & Becker, 2013; Marty, 2012; Peslier et al., 2017; Loewen et al., 2019).

The earliest known evidence for liquid water present on Earth's surface includes the Isua Greenstone Belt, where pillow-lava structures consistent volcanic eruption in submarine conditions occur as early as $\sim 3.8$ billion years ago (Polat & Hofmann, 2003). The presence of stable liquid water on Earth's surface marks a significant point in geological history, as the infiltration of water-rich mineral phases into the upper mantle reduced melting temperatures and led to the formation of the mechanically weak Astheno-

| Setting | $\delta$D [‰] | $^3$He/$^4$He [$R_A$] | Example | Reference |
|---|---|---|---|---|
| OIB | $< -75$ | $< 40$ | Iceland, Hawaii<br>Samoa, Galapagos<br>Easter | (Jackson et al., 2017)<br>(French & Romanowicz, 2015)<br>(Boschi et al., 2007)<br>(Poreda et al., 1986)<br>(Rison & Craig, 1983) |
| MORB | $-70$* | $7 - 9$ | Iceland<br>Mid Atlantic Ridge | (C. J. Allègre et al., 1995)<br>(Gautheron & Moreira, 2002) |
| Arc/back-arc | $-20$ to $-40$** | $\sim 1$*** | Valu Fa ridge<br>Andes | (Hilton et al., 1993) |
| CH | $-23$<br>to $-89$ | $8 - 20$ | Afar, Darfur<br>Hoggar | (Jimenez-Rodriguez et al., 2023)<br>(Jackson et al., 2017) |

**Table 1.** Typical isotope ratios of various tectonic settings. OIB = Ocean Island Basalt, MORB = Mid Ocean Ridge Basalt, CH = Continental hotspot. $\delta$D values are measured relative to Standard Mean Ocean Water (see text). $^3$He/$^4$He ratios are measured relative to present-day atmospheric values, $R_A$, where $R_A = 1.4 \times 10^{-6}$ (Graham, 2002). OIB settings supported by hotter mantle plumes with increased buoyancy are hypothesised to support increased transport of primordial or deep mantle material from the lower mantle to Earth's surface (Jackson et al., 2017). *Extremely low $\delta$D values of $< -90$ ‰ are observed in some MORBs associated with multi-stage melting and anhydrous minerals isotopic fractionation (see text) (Loewen et al., 2019). **High $\delta$D values in typical arc and back-arc settings ($< -20$‰) indicate the recycling of non-mantle water due to the subduction of hydrous minerals contained in the mantle wedge from beneath arc lavas, with lower $\delta$D values ($> -40$‰) associated with mixing with depleted mantle sources (Shaw et al., 2008). ***Igneous rocks from arc/back-arc settings not associated mantle mixing (i.e. differentiated silicic rocks) have negligible $^3$He/$^4$He ratios $\sim 1R_A$ (Hilton et al., 1993). Continental hotspots, most notably African examples, vary significantly from continental lithoshpere and differentiated back-arc basin igneous rocks. Mantle-supported continental hotspot have $^3$He/$^4$He ratios ranging from typical MORB values to $20R_A$ (Jackson et al., 2017).

sphere, and the onset of plate tectonics around $\sim 3$ billion years ago (Farquhar et al., 2002; Shirey & S.H., 2011; Debaille et al., 2013).

Since both helium and hydrogen are incompatible during mantle melting (i.e. both partition into a melt as soon as melting begins), high $^3$He/$^4$He ratios characterise a mantle that has been isolated from melting and degassing since the earliest stages of Earth history (C. Allègre et al., 1983; Mukhopadhyay, 2012; Loewen et al., 2019). Hence, rocks which contain low $\delta$D and high $^3$He/$^4$He signatures are a prime target for understanding sources of deep mantle water that has survived significant mixing and transport over planetary lengthscales (Craig & Lupton, 1976; Rison & Craig, 1983; Poreda et al., 1986; Loewen et al., 2019; Mackintosh & Ballentine, 2012).

Subduction zones represent the primary regions of terrestrial water exchange between Earth's interior and hydrosphere. It is estimated that $\sim 25\%$ of the water entering subduction zones reaches the transition zone and $\sim 3\%$ reaches the lower mantle through transport via lithosphere fragments (LF) that separate from subducted slabs (Figure 1) (Bodnar et al., 2013). Slab break-off and the transport of lithosphere fragments to the deep mantle has been investigated extensively, and is supported by plate tectonic reconstructions and geophysical data (e.g. (Williams & Hemley, 2001; Sperner et al., 2001; Zahirovic et al., 2016; Kufner et al., 2021)). It is impossible to know the precise amount

of lithospheric material that has been returned to the mantle over geologic time, however it is reasonable to imagine the presence of graveyards of remnant fossil lithosphere distributed heterogeneously throughout the mantle (e.g., van der Meer et al. (2018)).

The subduction of hydrous minerals and recycling of water into the mantle over geologic time and to the present day thus led to an increase in $\delta D$ in Earth's crust, upper mantle, oceans and atmosphere compared to primitive or lower mantle materials. Estimates of the water content within Earth range from $7-14$ $M_{oceans}$ within the mantle and $< 12$ $M_{oceans}$ in the core (Bodnar et al., 2013; Nestola & Smyth, 2016; Peslier et al., 2017). Hence, subuduction and lithosphere fragments have a profound impact on the dynamics of mantle convection and Earth's hydrogen cycle the through mixing of non-mantle material into deep mantle reservoirs.

As Earth's crust and tectonic processes evolved, the planet's atmosphere also underwent significant changes that impacted the stability of water and hydrogen generative processes on Earth's surface. Dodd et al. (2022) investigated hydrogen dynamics before and after the Great Oxidation Event (GOE) at $\sim 2.5 - 2.0$ Ga. Initially, abiotic reactions in anoxic conditions led to hydrogen generation from banded iron formations (BIFs), with free hydrogen escaping due to low oxygen levels. As the concentration of biologically generated $O_2$ within Earth's atmosphere gradually increased, the atmosphere changed from weakly reducing conditions and practically devoid of oxygen into oxidising conditions, and containing abundant free oxygen Torres et al. (2015). Post-GOE, elevated oxygen facilitated water formation by reacting with hydrogen, reducing hydrogen escape and transitioning Earth to a more oxidised state supportive of aerobic life and altering geochemical dynamics significantly (Dodd et al., 2022).

Present-day patterns of high-angle subduction and mantle wedge hydration (i.e. as shown on Figure 1) were not dominant during the early Earth, as most present-day subduction initiation mechanisms require acting plate forces and existing zones of lithospheric weakness, which are both consequences of plate tectonics. In the absence of plate tectonic-related subduction, mechanisms responsible for the initiation of tectonics during early history are theorised to be plume-induced subduction, which is only feasible in the hotter early Earth for old oceanic plates. In contrast, younger plates favoured episodic lithospheric drips rather than self-sustained subduction and global plate tectonics (Gerya et al., 2015). It is possible that the development of the modern, globally interconnected plate network and subduction-related tectonics did not arise until billions of years after the formation of the earliest crust and as late as Proterozoic times (Wan et al., 2020). This assertion is consistent with modeling studies that demonstrate that much of the continental crust of Archean cratons could have been generated in the absence of subduction (Capitanio et al., 2019; Johnson et al., 2017).

However, some evidence indicates localised infiltration of hydrated mantle wedges into the mantle occurred as early as 3.1 Ga, there is a consensus in the literature that higher mantle temperatures, lower mantle viscosity and the subduction or infiltration of oceanic crust at an unusually low angle was responsible for the growth of continental crust older than $\sim 2.5$ Ga (e.g., Perchuk et al. (2023); Smithies et al. (2003)). Although, it is important to note that a hotter mantle would lead to lower viscosity and thus more melt, with the lower viscosity leading to more frequent slab breakoff, and to increased crustal separation from the mantle lithosphere (van Hunen & van den Berg, 2008). Crustal and lithospheric fragments which break off, contaminate, and sink into the mantle raise $\delta$D and lower $^3He/^4He$ ratios over geologic time away from primordial or lower mantle values and towards their present-day values. Therefore, it is our view that whilst localised tectonic processes early in Earth history will have had some impact on the distribution of hydrogen within the mantle, the onset of global subduction marked the turning point of large-scale mantle mixing leading to present-day heterogeneous mantle hydrogen contents. Throughout Earth history, plume-related tectonics will have been

responsible for transporting material enriched in primordial or lower mantle hydrogen and helium to the surface on geologically short timescales.

## 3 Hydrogen in the shallow Earth

Whilst the migration of hydrogen in the deep Earth is dependent on large-scale mantle convective and tectonic processes that operate from billions to millions of years, the enrichment of hydrogen within near-surface systems and ongoing emission from surface seeps across the globe represents an intriguing duality of length-scales and timescales. Shallow Earth processes, such as the migration in porous media, migration along faults and fractures and microbial reactions may operate over timescales of thousands of years to hours. To understand hydrogen migration in the shallow Earth, we must acknowledge the relationship between hydrogen sources and transport mechanisms at the crustal, basin and outcrop scale, i.e. $10^3 - 1$ m. The primary mechanisms of natural hydrogen generation are thought to be: (1) serpentinisation of mafic rocks, (2) radiolysis of water, (3) rock fracturing and (4) volcanic degassing, (5) maturation of organic matter and (6) weathering of iron-rich rocks (Takai et al., 2004; Klein et al., 2013; Zgonnik, 2020; Lefeuvre et al., 2021, 2022; Geymond et al., 2022; Horsfield et al., 2022; Mahlstedt et al., 2022; Boreham et al., 2023; L. Wang, Jin, et al., 2023).

However, to date a distinction between processes that release primordial or deep mantle (i.e. fossil) hydrogen and the chemical and biological production/destruction of 'new' hydrogen is seldom made in the literature. Hydrogen gas concentrations of $> 10\%$ have been encountered in various locations across different tectonic regimes (see ? (?)) with one documented case of a successful resource discovery in Mali (Prinzhofer et al., 2018). The mineralogies of Archaen - Proterozoic basement rocks in continental cratonic regions (e.g. Africa, Brazil, Russia) and mantle-derived rocks (e.g. MORBs, OIBs) are enriched in hydrogen. Hence, within the continental realm, regions of high hydrogen concentration coincide with sedimentary basins underlain by Archean - Proterozoic cratonic rocks enriched in hydrogen (Zgonnik, 2020; Moretti, Brouilly, et al., 2021). Early estimates of global hydrogen production rates via both radiolysis and hydration reactions from the Precambrian continental lithosphere were reported at $0.36{-}2.27{\times}10^{11}$ moles/year and are comparable to estimates from marine systems (Lollar et al., 2014). As recent literature has reviewed the topic of natural hydrogen generation extensively (e.g. Zgonnik (2020); Moretti, Brouilly, et al. (2021); L. Wang, Jin, et al. (2023)), we limit our coverage of this topic and focus on the relationship between natural hydrogen generation and its migration pathways to Earth's surface. In this section, we review the mechanisms and timescales of transport of hydrogen within diffusive and advective systems, including transport along faults and microbial reactions, within the shallow Earth.

### Diffusion

#### *Diffusion in crystalline rocks and minerals*

Diffusive mechanisms transport hydrogen without any motion of a material's bulk (e.g. rock, crystalline matrix or fluid). Experimental results of hydrogen diffusivity within crystalline rocks are reviewed extensively by Farver (2010); Demouchy (2010); Li and Chou (2015) (see references therein) and summarised in Figure 2. Within the primary mafic rock-forming minerals olivine, pyroxene and amphibole, the Arrhenius plots of Farver (2010) indicate a pattern of decreasing hydrogen diffusivity from $10^1$ cm$^2$/year to $10^1$ mm$^2$/10 ka with decreasing Mg content. Hydrogen diffusivity within quartz and feldspar vary between $10^1$ cm$^2$/year to $10^1$ cm$^2$/ka, however have been measured up to 1 m$^2$ yr$^{-1}$ - 1 m$^2$ day$^{-1}$ in the case of fused quartz at temperatures $> 1200$ K (Li & Chou, 2015). Oxide minerals, which are significant components of soils and regolith, along with metamorphic minerals (e.g. garnet) have hydrogen diffusivities of $10^1$ cm$^2$/year - $10^1$ cm$^2$/ka (Figure 2B). A strong relationship between mineral structure and hydrogen diffusivity

is also seen (Figure 2C). Experiments by Kohlstedt and Mackwell (1998); Demouchy and Mackwell (2006); Demouchy (2010) show a clear distinction between hydrogen diffusivity within crystalline aggregate and at grain boundaries (Figure 2D). For olivine, hydrogen diffusivity at grain boundaries is measured at $\sim 1$ m$^2$ year$^{-1}$, which can be considered instantaneous given an average grain boundary thickness of 0.75 nm (Demouchy, 2010).

Whilst such experimental results show that hydrogen diffusivity at grain boundaries and within mineral aggregates (e.g. fused quartz) may be significant, this is outweighed by exponentially decreasing diffusivity with increasing grain size (Figure 2E). Grain sizes for crystalline rocks are a function of their cooling histories, with cratonic crystalline basement and mantle xenoliths exhibiting average grain sizes from millimetres to several centimeters. However, individual crystals can reach up to 30 cm in size in some ultramafic mantle xenoliths with prolonged cooling histories (Hoskin & Sundeen, 1985; Speciale et al., 2020; Sharapov et al., 2022)). Furthermore, the maximum temperatures of diffusivity experiments ($< 1600$ K) are representative of mantle conditions and not encountered within the continental realm and sedimentary basins, which typically vary between $\sim 300-500$ K (Hantschel & Kauerauf, 2009). The exponential relationship of Demouchy (2010) indicates a decrease in hydrogen diffusivity of $\sim 3$ orders of magnitude between grain sizes of 10 mm and 0.1 mm, at which point the relationship flatlines. Given these experiments were conducted at a pressure and temperature representative of upper mantle conditions, it is reasonable to assume that the diffusivity of olivine (and other minerals) at typical continental and sedimentary basin conditions will be many orders of magnitude smaller than the measurements of Demouchy (2010). Given these factors, experimental results indicate that native hydrogen entrained within the mineral structure of crystalline rocks within the shallow Earth may diffuse on geological timescales from the most common rock forming minerals. Geochemical data obtained by Parnell and Blamey (2017) indicate that common felsic lithologies, such as granites, gneiss and conglomerates of Archean - Proterozoic ($> 1600$ Ma) age consistently contain an order of magnitude greater hydrogen concentration in their entrained fluid than very young ($< 200$ Ma) granites. Parnell and Blamey (2017) found that sedimentary rocks containing clasts of old basement also included a greater proportion of hydrogen than young granites and hypothesise that a signature of hydrogen in the basement could be conferred to the sediment and that modern sediment derived from old and young basement retains the signature of more or less hydrogen, respectively. It should be noted, however, that the experimental results summarised by Parnell and Blamey (2017) refer to bulk lithologies whereas those of Farver (2010) refer to individual minerals (e.g. olivine and quartz). Furthermore, the preservation of high hydrogen abundances within fluid inclusions and mineralised veins in ancient granites has been observed (Bourdet et al., 2023). Hence, diffusion from enriched Archean - Proterozoic crystalline basement may supply a 'background' hydrogen flux to overlying sedimentary basin rocks on geological timescales. Hydrogen diffusion from coarse grained crystalline rocks, e.g. crystalline basement, granites and their derived sedimentary products, e.g., conglomerates, must operate on timescales of Ma - Ga in order to explain the provenance of high hydrogen signatures in sedimentary rocks that contain material sourced from enriched Archean - Proterozoic basement. This is consistent with the widely documented observation of higher hydrogen fluxes in sedimentary basins in continental cratonic regions underlain by Archean - Proterozoic basement (e.g. Zgonnik (2020); Moretti, Brouilly, et al. (2021)). In the case of rapidly cooled upper mantle rocks, e.g. MORBs, volcanic glasses, pillow lavas, however, grain sizes may be many orders of magnitude smaller than their continental counterparts and within the nanometre scale (e.g., Schlinger et al. (1988)). Hence, hydrogen diffusivity in rapidly cooled crystalline rocks and at MOR settings will be significantly faster than in continental settings and potentially only a few orders of magnitude slower than the lower temperature ranges of diffusivity experiments, i.e. 100 Ka - Ma or faster. This is significant, since the age of most oceanic crustal rocks is $< 60$ Ma (Seton et al., 2020), hydrogen diffusion within oceanic crustal rocks will operate on the same timescale

as the age of rocks themselves and provide a mechanism for the degassing of mantle hydrogen to the surface and oceans.

### *Diffusion in sedimentary rocks*

The rate of hydrogen diffusivity in sedimentary rocks is dependent on a wide range of factors, including lithology, porosity, permeability, temperature, pressure, salinity and water content. Typical values for hydrogen diffusivity in different sedimentary rocks, water and air are summarised in Table 2

Unlike for crystalline rocks and minerals, hydrogen diffusivity experiments for sedimentary rocks are carried out at temperature and pressure conditions representative of sedimentary basins. These are typically at temperatures between $288-413$ K and pressures $< 40$ MPa. A strong positive temperature dependence is seen in silt, clay, coal, shale and salt, whereby hydrogen diffusivity values vary by $> 50\%$ over a narrow range of $\sim 40$ K (C. Wang et al., 2024; J. Liu et al., 2022; Keshavarz et al., 2022; Vinsot et al., 2014). Hydrogen diffusivity decreases with increasing pressure, owing to increased fluid density at the same temperature and fixed space causing gas diffusion to be restrained (J. Liu et al., 2022). Measurements by J. Liu et al. (2022) of density profiles of hydrogen in silt (montmorillonite) corresponding to different pressures indicate that the mineral adsorption layer is not influenced by increasing pressure, thus causing pressure to have an important but albeit lesser, effect on hydrogen diffusivity than temperature. At experimental conditions of 353 K and 10 MPa, a reduction in hydrogen diffusivity of $\sim 50\%$ at a threshold water content of $\rho^{ave}_{H_2O} = 0.568$ gcm$^{-3}$, and $\sim 12\%$ as salinity increases from $8-12$ wt% is observed in silt (J. Liu et al., 2022). This may be explained by the effects of increasing water content and salinity on the geometry of brine-rock and brine-hydrogen molecule contacts. When water content and salinity are low, hydrogen and brine form a stratified structure and the diffusivity of hydrogen is similar to that of confined pure gas at the same pressure and temperature conditions. Increasing water content and salinty leads to increased connectivity of brine molecules, the formation of water bridges between brine molecules and mixing of hydrogen and brine as a new phase, leading to a decrease in hydrogen diffusivity by up to 5 orders of magnitude (Figure 3, J. Liu et al. (2022)). Measurements of both dry and water-wet samples of various rock types by (Strauch et al., 2023) indicate that hydrogen diffusivity decreases further by an order of magnitude due to the effect of fracture healing with increased water content (Strauch et al., 2023). Hydrogen breakthrough times vary significantly with water content, most notably for salt rocks whereby values increase from $1 - 843$ hours.

Measurements of $H_2-$brine contact angles versus pressure and total organic carbon (TOC) in various water-wet Australian antracite shales by Al-Yaseri et al. (2022) indicate that capillary entry pressure decreases with increasing pressure and TOC, thus leading to a reduction in sealing capacity with depth and TOC. Within salt, hydrogen diffusion is strongly dependent on mineralogy, crystal shape and size. Diffusion through intact halite crystals with no discontinuities is negligible, whilst salt crystal boundaries and fractures within grains are the preferential flow paths for gas diffusion (Yuan et al., 2023).

Whilst hydrogen diffusivity experiments offer an insight into the absolute timescale of hydrogen migration through different materials, a more useful measure of sealing ability is the breakthrough time. The breakthrough time, $t_b$ is defined as the time interval between the start of gas purging of the feed chamber and the first detection of hydrogen at the sensor in the permeate chamber. Whilst there are various methods to calculate $t_b$, the time-lag method of Frisch (1957) is widely applied due to its practicality and ability to allow for the transient definition of a microstructure dependent correlation of breakthrough time and sample thickness (Rhode et al., 2022). From Frisch (1957), $t_b \sim$

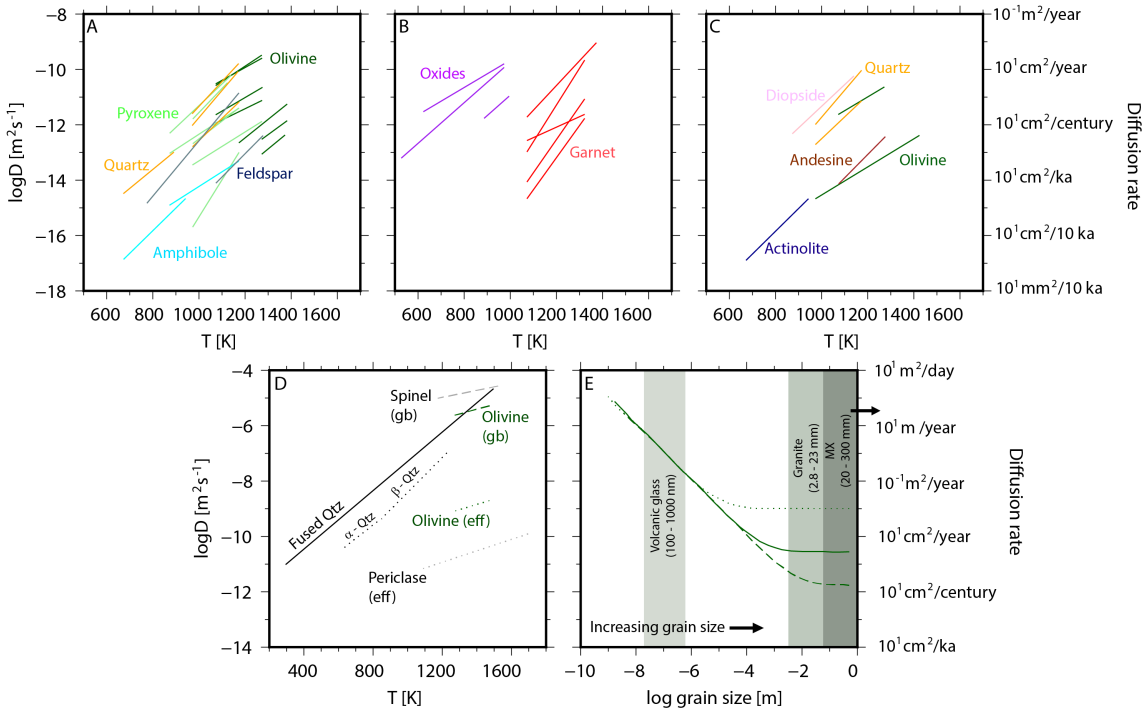


**Figure 2.** Hydrogen diffusivity as a function of mineralogy and lithology. A = Hydrogen diffusivity in the primary rock-forming minerals. These minerals constitute a significant component of Archean - Proterozoic crystalline basement (both mafic and felsic). B = Hydrogen diffusivity in oxides and garnets. C = Hydrogen diffusivity in different mineral structures. Whilst hydrogen diffusivity varies significantly with mineral structure, there is no obvious relationship between the two. D = Hydrogen diffusivity in fused, $\alpha$ and $\beta$ quartz from (Li & Chou, 2015). Effective diffusivity in and diffusivity at grain boundaries (gb) for olivine, spinel and periclase from (Demouchy, 2010). Diffusivity at gb are several orders of magnitude greater than within crystal lattices. E = Hydrogen effective diffusivity in olivine aggregate at 1473 K and 300 MPa and grain boundary width = 0.75 nm (Demouchy, 2010). Hydrogen diffusivities are calculated using the gb diffusion from (Demouchy, 2010) and the "proton-vacancy" mechanism for lattice diffusion in olivine along [001] (dashed line) and along [100] and [010] (dotted line, Demouchy and Mackwell (2006) and "proton–polaron" mechanism for lattice diffusion in olivine along [100] (solid line, Kohlstedt and Mackwell (1998)). Diffusivity decreases exponentially with grain size. Grain size ranges for plutonic granites and mantle xenoliths (MX) are shown in medium and dark grey (Hoskin & Sundeen, 1985; Speciale et al., 2020). Black horizontal arrow indicates MX grain sizes beyond the axes range (e.g., Sharapov et al. (2022)). Typical grain sizes for microcrystalline volcanic glasses vary from 100 – 1000 nm and are shown in light grey (Schlinger et al., 1988). Diffusivity data from Farver (2010) (A-C), citetDemouchy2010, Li2015 (D-E). Panel E modified from Demouchy (2010).

| Rock type | Diffusivity [$m^2s^{-1}$] | $t_{b_1}$ (dry) [years] | $t_{b_1}$ (wet) [years] | Reference |
|---|---|---|---|---|
| Bentheimer sandstone | $1.6 - 2.1 \times 10^{-9}$ | 2.5 | 3.3 | Strauch et al. (2023) |
| Silt (montmorillonite) | $4.25 - 8.27 \times 10^{-8}$ | 0.06 | 0.12 | (J. Liu et al., 2022) |
| Opalinus Clay | $1.2 - 5.13 \times 10^{-9}$ | 1.0 | 4.4 | Vinsot et al. (2014)<br>Strauch et al. (2023) |
| Coal (anthracite) | $1.3 - 7 \times 10^{-8}$ | 0.08* | 0.52* | Bagreev et al. (2004),<br>Keshavarz et al. (2022) |
| Shale | $1.3 - 2.4 \times 10^{-8}$ | 2.2 | 3.7 | Al-Yaseri et al. (2022) |
| Werra rock salt (halite) | $1.4 \times 10^{-9} - 1.3 \times 10^{-8}$ | 0.40 | 3.7 | Strauch et al. (2023) |
| Water (pure) | $3.9 - 6.1 \times 10^{-9}$ | | | de Blok et al. (1982)<br>Ferrell and Himmelblau (1967)<br>Jacops et al. (2017)<br>Hemme and van Berk (2018) |
| Air | $0.756 - 1.604 \times 10^{-4}$ | 0.3 hours | 0.6 hours | Mostinsky (2011)<br>ToolBox (2018) |
| Stainless steel | $1.5 \times 10^{-11}$ | 352 | | Owczarek and Zakroczymski (2000) |

**Table 2.** Hydrogen diffusivity values for various sedimentary rock types and materials and breakthrough times through 1 m of material, , $t_{b_1}$, estimated using the time-lag method (see body text). Hydrogen diffusivity experiments for sedimentary rocks are conducted at temperatures and pressures representative of sedimentary basin conditions and are much lower than experimental conditions used for crystalline rocks and minerals. Variation in diffusivity values are due to dry and wet samples. The temperatures and pressures applied to the experimental results summarised in this table vary between 288 $-$ 413 K and $<$ 40 MPa, respectively. The diffusivity of hydrogen in pure water, air and stainless steel are included for reference. *Due to lack of available date in the literature, values for coal are estimated using $H_2S$ diffusivity measurements (Bagreev et al., 2004).

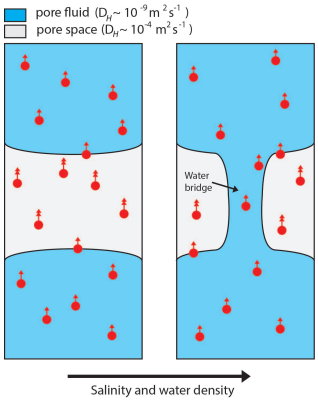


**Figure 3.** Effects of increasing salinity and water density on hydrogen diffusivity. Increasing salinity and density of pore fluid within sedimentary rocks leads to the formation of water bridges and increased connectivity between brine molecules, inhibiting the diffusion of hydrogen. Red circles = hydrogen molecules. Diffusion rates of hydrogen ($D_H$) in air are up to five orders of magnitude greater than in water and are indicated by double and single arrows, respectively. Modified from (J. Liu et al., 2022)

$L^2/6D_H$, whereby $L$ = length of sample thickness. Hence, the breakthrough time through 1 m of rock may be approximated as $t_{b_1} \sim 1/6D_H$.

Using published values, estimated $t_{b_1}$ values for sedimentary rocks are shown in Table 2. $t_{b_1}$ values are on the scale of years for dry and wetted rock samples, with breakthrough times for wetted rocks typically several times greater than for dry rocks (Strauch et al., 2023; J. Liu et al., 2022; Vinsot et al., 2014; Keshavarz et al., 2022; C. Wang et al., 2024; Al-Yaseri et al., 2022; de Blok et al., 1982; Ferrell & Himmelblau, 1967; Jacops et al., 2017; Hemme & van Berk, 2018; Mostinsky, 2011; ToolBox, 2018; Owczarek & Zakroczymski, 2000).

### Advection

Advection is the transport of a substance due to the motion of a carrier, e.g. water. In the case of hydrogen, gaseous $H_2$ may also be carrier for itself. Advective transport systems within the subsurface include fluid migration along faults and discontinuities and groundwater flow through aquifers and are summarised on Figure 7. By its nature, the advection of hydrogen through sedimentary basins is a complex process that cannot be described in a single step. A hydrogen molecule may migrate from depth to the surface through a combination of the mechanisms shown on Figure 7 and diffusion during these processes.

#### *Migration in porous media*

Migration through porous sedimentary rocks is one of the most significant mechanisms of fluid transport within sedimentary basins across the world. Fluids, such as hydrocarbons and $CO_2$, displace and interact with formation fluids present within the pore spaces in sedimentary rocks, with flow directed along pressure gradients exerted on the system. In the case of hydrogen, transport via dissolution in groundwater within aquifers is one of the primary mechanisms of advective migration in the shallow Earth. Natural hydrogen migration via transport within sedimentary rocks and groundwater has not received much attention in literature and is not yet well understood. It is however known

to be affected by factors such as salinity, temperature, pressure, formation fluid composition and fluid-rock interactions.

Shallow aquifers have typical depths from near-surface to $\sim$ 100 m, whilst deep aquifers may reach up to 9000 m. Temperature and salinity ranges in aquifers vary between $7-174$°C and $5-52000$ ppm, respectively (Dopffel et al., 2021). These factors exert a primary control on both the solubility of hydrogen in groundwater and microbial abundance and activity, which have important implications for hydrogen migration (e.g. Berta et al. (2018); Koproch et al. (2019)). Similar to other gases, the solubility of hydrogen in water decreases proportionally with salt (NaCl) concentration, until the solution is saturated (Chabab et al., 2020). Recent solubility data of hydrogen in water-brine under geological conditions typical of aquifers were used by Chabab et al. (2020) to determine empirical relationships between hydrogen solubility and salt concentration in pure water and brine with 0.5−2% Average Absolute Deviation to observed values. These are:

$$x^0_{H_2} = b_1 PT + \frac{b_2 P}{T} + b_3 P + b_4 P_2 \tag{1}$$

for pure water at $273.15 < T < 323.15$ K and $0.1 < P < 20.3$ MPa, and

$$ln\left(\frac{x_{H_2}}{x^0_{H_s}}\right) = a_1 m^2_{NaCl} + a_2 m_{NaCl} \tag{2}$$

for brine at $323.15 < T < 373.15$ K, P $1 < P < 23$ MPa and $m_{NaCl} < 5$ mol/kg, whereby $T$ = temperature, $P$ = pressure, $X_{H_2}$ = hydrogen solubility, $x^0_{H_2}$ = hydrogen solubility in pure water, $m_{NaCl}$ = molality of salt and $a_i$, $b_i$ = empirical coefficients listed in (Chabab et al., 2020). The amount of dissolved hydrogen decreases with increasing salinity (see Figure 9 Chabab et al. (2020)). New measurements of hydrogen solubility carried out under conditions of high pressure (< 20 MPa), temperatures ranging from 298−373 K and salinities < 4 mol/kgw of NaCl by Chabab et al. (2024) indicate that $H_2$ solubility in water and brine increases with pressure and follows Henry's law in a quasi-linear trend. Models optimised on experimental data predict a minimum solubility temperature ($T_{xH2,min}$) of around $\sim$ 326 K in pure water, decreasing with salinity ($T_{xH2,min}$ = 315K at 2 molal NaCl and $T_{xH2,min}$ = 288K at 4 molal NaCl) (Chabab et al., 2024).

The interaction between natural hydrogen and resident formation fluid, e.g. water, present within the pore spaces of sedimentary rocks is also of significance as this influences the displacement of the former over the latter within geological porous media. Measurements of hydrogen-brine interfacial tension, $\gamma$, over a wide range of $T$, $P$ and $m_{NaCl}$ ranges by Hosseini et al. (2022) indicate an inverse linear relationship between $\gamma$, $P$ and $T$. $\gamma$ was found to have a strong dependence on temperature, and decreased linearly at constant pressures and salinity. $\gamma$ increased significantly and linearly with increasing salinity at constant temperatures and pressures, whilst decreasing at a lower rate with increasing pressure at constant temperature and salinity due to the increasing intermolecular forces between hydrogen and water at elevated pressures (Iglauer et al., 2012; Hosseini et al., 2022). Hence, temperature and salinity have a greater effect than pressure on the solubility of hydrogen and its ability to displace formation fluids within porous media (Hosseini et al., 2022; J. Liu et al., 2022). With regards to diffusivity, simulations of molecular dynamics at subsurface conditions conducted by Kalati et al. (2024) indicate lower diffusivity at higher salinity and lower temperature, the value being $7.29\times 10^{-9}$ m$^2$/s at 323 K, increasing to $10.2\times10^{-9}$ m$^{-2}$/s at 353 K for 1 molal NaCl solution. The diffusion coefficient decreases up to 38% as the salinity increases from 1 to 5 molal (Kalati et al., 2024). The results of Kalati et al. (2024) correspond to simulation

results by Lopez-Lazaro et al. (2019), which measure the temperature minimum hydrogen solubility close to 326 K.

### *Migration along faults and fractures*

The episodic circulation of fluids and gases along geological faults is intricately controlled by mechanisms governing fault opening and sealing, as well as the timing of these processes. Fluid advection along crustal faults is a well-documented phenomenon (Cox & Etheridge, 1989), and it is a recurrent occurrence in the Earth's crust (Marques et al., 2018). These faults play a pivotal role in the migration of gas such as hydrogen, serving as both conduits and barriers. Studies at both reservoir and basin scales have demonstrated that fault transmissivity is primarily influenced by (i) the fault's type, geometry, and displacement; (ii) the internal architecture of the fault zone; (iii) the surrounding stratigraphy and lithology; and (iv) the geomechanical stress (Faulkner et al., 2010; Solum et al., 2010; Massiot et al., 2019). Due to the variability of these parameters, fault transmissivity evolves both temporally and spatially (Frery et al., 2015; Frery, Fryer, et al., 2021). The opening of faults can be triggered by seismic events, fluid overpressures, or localised dissolution (Gratier & Gueydan, 2007), while their closure can be attributed to progressive sealing resulting from mechanical (Hancock et al., 1999; Eichhubl & Boles, 2000), chemical processes and fault roughness (Renard et al., 2013).

Fault zones are complex features that can be effectively modelled as damaged zones and gouges with heterogeneous porosity and permeability architectures. For instance, in the North Perth Basin (Australia), these fault zones exhibit a highly compartmentalised nature, primarily acting as barriers to crossflow while driving upward fluid migration. This structural configuration provides an ideal setting for structurally controlled hydrogen migration (Frery, Langhi, et al., 2021). For instance, above a natural subsurface CO2 reservoir, a causal relationship between $CO_2$ pulsing and fault opening have been demonstrated using isotopic analysis (C, O, Sr ratios, Ba/Ca, and Sr/Ca elemental ratios)(Kampman et al., 2012). The opening of veins is associated with a pulse of $CO_2$ within the system, followed by a degassing phase that occurs simultaneously with vein growth. Consequently, abrupt events may have triggered the opening of fractures, immediately followed by episodes of fluid circulation. Evidence of fault opening events can be observed with durations ranging from millennia to centuries (Burnside et al., 2013; Frery et al., 2015; Gratier & Gueydan, 2007).

In regions of active faulting, stress cycling and the creation and destruction of permeability and fluid flow are closely linked . Both large (km) and small-scale (¡ m) faults are capable of influencing fluid migration pathways within sedimentary basins. The advection of hydrogen-enriched fluids along large-scale faults are attributed to natural hydrogen fluxes recorded in several well-known case studies, including Mali, Brazil and the north Pyrenees (France) (Prinzhofer et al., 2018; Myagkiy, Brunet, et al., 2020; Donzé et al., 2020; Lefeuvre et al., 2022). Common factors include the intersection of deep, crustal-scale faults with Archean-Proterozoic crystalline basement or ultramafic mantle bodies that are serpentinised, hydraulic or elevated temperature and pressure gradients that trigger fluid migration. Measured daily flow rates of gaseous $H_2$ flux within fault zones by Lefeuvre et al. (2022) ranges from $0.07{-}0.15$ $m^3m^{-2}d^{-1}$ in the north Pyrenees. These values are comparable to measurements of gaseous $H_2$ flux within soils from the Sao Francisco basin in Brazil and the Semail ophiolite, Oman (Prinzhofer et al., 2019; Zgonnik, 2020; Moretti, Prinzhofer, et al., 2021). The measurements of Lefeuvre et al. (2022) equate to a timescale of $\sim 128 - 274$ years for hydrogen migration over a distance of $\sim 7$ km from its serpentinite source to trap beneath a clay-rich seal. Templeton et al. (2024) note that whilst low temperature water-rock reactions produces net $H_2$ from the oxidation of Fe(II)-bearing minerals within the Semail Ophiolite, biological activity is predicted to be stimulated by fluxes of $H_2$, giving rise to net $H_2$ consumption. The most probable detection of $H_2$ at the surface is at hyperalkaline seeps sourced by deep faults, rather

than in most soils and peridotite outcrops, due to efficient microbial $H_2$ scavenging of the available $H_2$ flux in the upper aquifer, where measured $H_2$(aq) levels drop below detection (Templeton et al., 2024). Hence, from a migration perspective it is reasonable to hypothesise that the migration of hydrogen-rich fluids along faults within the upper several kilometers of the subsurface in this instance must occur over a timescale of hours to days, and must be faster the timescales of biogenic reactions responsible for hydrogen consumption.

Aside from large-scale faulting, complex networks of small-scale (10−100 m throw) faults restricted to individual sedimentary layers, known as polygonal fault systems (PFS) have been identified as having important impacts on basin-scale fluid flow. The impact of PFS on fluid migration is debated within the literature, with authors attributing PFS for both enhancing (e.g., Ireland et al. (2021); Cartwright (2011); Cartwright et al. (2003)) and restricting (e.g., Xia et al. (2022); Andresen and Huuse (2011)) fluid flow. Whilst PFS have been identified as a mechanism for seal bypass (Ireland et al., 2021), permeability may be effectively destroyed by clay smearing along fault planes and thus increase the sealing capacity of PFS (Xia et al., 2022; Andresen & Huuse, 2011). Basin inversion, fault reactivation or dewatering of host sediments may lead to the periodic opening of fluid, and thus hydrogen migration pathways along impermeable PFS (Xia et al., 2022). Whilst PFS must inevitably enhance the passage of fluids during their diagensis, it is unlikely that PFS and microfractures provide substantial hydrogen migration pathways over geological timescales during periods of tectonic quiescence. However, PFS may be capable of both providing a mechanism for fluid communication and opening hydrogen migration pathways on short geological timescales during periods of tectonic activity or fault slip.

Whilst faulting and fluid flow have been extensively reviewed in the literature, their impact on hydrogen migration have only recently gained significant attention. Early work by by Wakita et al. (1980) hypothesised the production of hydrogen by fault movement, based on measurements of elevated hydrogen concentrations ($> 3\%$ by volume) around active fault zones in southwestern Japan compared to background measurements of $\sim$ 0.5 ppm. Su et al. (1992) identified the potential reduction in strength of crystalline minerals (e.g., calcite, dolomite, antigorite) due to hydrogen infiltration at low pressures, leading to the weakening of rocks and initiation of faulting. Hydrogen gas measurements and particle size distribution analyses by Niwa et al. (2011) within an active fault zone indicate that hydrogen gas mostly migrated in permeable fracture zones by advection with groundwater. Firstov and Shirokov (2005) measured seven pulses of hydrogen discharge against background levels in a fault zone trending parallel the Kuril - Kamchatka geostructural zone, Russia, from 1999−2003. Hydrogen pulses preceding seismic events lasted from 1.5−6 hours and were 2−14 times higher than measured background levels. Firstov and Shirokov (2005) found that $< 80\%$ earthquakes with $M_W \geq 5.6$ in the southern Kamchatka region occurred within one month of measured hydrogen pulses and considered such events as short-term earthquake precursors. In recent years, the migration of natural hydrogen from deep crustal sources along kilometre-scale faults which penetrate crystalline basement have been recorded in several locations across the world (e.g., Brazil, France, Mali) (Prinzhofer et al., 2018; Deronzier & Giouse, 2020; Donzé et al., 2020; Rezaee, 2021; Frery, Langhi, et al., 2021; Lefeuvre et al., 2021, 2022).

***Surface seeps***

Surface hydrogen emissions are associated with a wide range of geological conditions, including serpentinised mafic rocks, rift zones, Precambrian rocks, volcanic rocks, volcanic gases, geysers, hot springs, mud volcanoes and isolated seeps. The emission of natural hydrogen and gas from surface seeps has been recognised for millennia, e.g., the continuously burning Olympic flame at Mount Olympus, Turkey, dating back 2500 years and comprised of 7.5−11.3% $H_2$ (Hosgörmez, 2007). Other examples include 'Los Fue-

| Type | Example | Characteristics | Reference |
|---|---|---|---|
| $H_2-$rich | 'Los Fuegos Eternos', Philippines | Noble gas signatures similar to air, pH< 10 | Vacquand et al. (2018) Abrajano et al. (1990) |
| $N_2-$rich | Semail, Oman | Ophiolitic, $^3He/^4He < 1R_A$ | Sano et al. (1993) |
| $N_2-H_2-CH_4$ | New Caledonia | Ophiolitic, mixing of $CH_4-H_2$ and $N_2-$rich components | Deville and Prinzhofer (2016) |
| $H_2-CH_4$ | Mount Olympus, Turkey Zambales, Philippines | Ophiolitic, active subduction, $^3He/^4He > 1R_A$ | Abrajano et al. (1988) Hosgörmez (2007) |

**Table 3.** Characteristics of surface abiogenic hydrogen seeps compiled from various references.

gos Eternos' (the eternal flames), discovered in the Philipines over two centuries ago with $H_2$ concentrations of 41.4−44.5% (Vacquand et al., 2018; Abrajano et al., 1990). The distribution of surface hydrogen seeps across the globe are reviewed extensively by Zgonnik (2020), and can be separated into four broad categories (Table 3).

A common characteristic of most abiogenic natural hydrogen seeps is an association with ultramafic rocks, ophiolites and serpentinisation. The hydrolysis and oxidation of primary ferromagnesian minerals, such as olivine and pyroxenes, produces $H_2$ over a wide range of environmental conditions (Holm et al., 2015). Elevated isotopic signatures, i.e. $^3He/^4He < 1R_A$, within hydrogen-rich fluids encountered at such surface seeps owe their provenance to primordial or deep mantle enrichment within ultramafic hydrogen source rocks. However, whilst the advection of hydrogen entrained within ultramafic rocks occurs over undoubtedly geological timescales, its liberation and transport to the surface must depend on the parameters driving the $H_2-$forming serpentinisation reaction. Measurement of $H_2$ degassing using in-situ gas chromatography and analysis of experimental products using XRD, Raman and X-ray absorption spectroscopy under serpentinisation conditions (300°C and 30 MPa) show a three stage process during the serpentinisation reaction: early ($0-18$ days), intermediate ($18-34$ days) and late ($34-70$ days). At the earliest stage, hydrogen is generated due to the crystallisation of magnetite, with Fe-rich serpentine also formed as a reaction product of olivine, enstatite, clinopyroxene and water. As the reaction progresses during the intermediate phase, hydrogen is generated due to the formation of serpentine and clinopyroxene is absent from the reaction. During the final stages of serpentinisation, the serpentinisation front has effectively disappeared and hydrogen is generated due to the oxidation of Fe-rich serpentine (Figure 4A, Table 4, Marcaillou et al. (2011)). The results of Marcaillou et al. (2011) are further supported by Greenberger et al. (2015), who investigated the progression of serpentinisation by mapping Fe oxidation states and analysing stable isotopes of carbon and oxygen in carbonates to constrain the conditions of water–rock interaction during serpentinisation. As groundwater migrates through a rock volume, the area of contact between ultramafic source rocks (e.g., harzburgite, olivine) and migrating fluids, i.e. serpentinisation front, is greatest at early stages of serpentinisation. The serpentinisation front is reduced as the reaction progresses, with maximum $H_2$ generation at the earliest stages of serpentinisation (Figure 5B Greenberger et al. (2015)).

Within subduction-related and ophiolitic terrains, all four types of seeps listed on Table 3 are encountered. However, the nature of gases and gaseous mixtures emitted at surface seeps is dependant on geodynamic context and the proportionality of mixing between different fluids. Noble gases display signatures close to the value of air in $H_2$-rich seeps, indicating that hydrogen gas emitted from ophiolitic settings is generated at shallow depths within Earth's crust. $N_2$-rich seeps are notably associated with relatively high contents of crustal $^4He$, and the source of $N_2$ is interpreted as derived mainly from metamorphosed sediments located on the subducted crustal slab, below the ophiolitic units

| Stage | Reaction | Reaction time |
|---|---|---|
| Early | Olivine + enstatite + cpx + $H_2O$ + $H^+$ → Serpentine + magnetite + $Mg^{2+}$ + $Ca^{2+}$ + $SiO_2$ + $\mathbf{H_2}$ | $0-18$ days |
| Intermediate | Olivine + enstatite + $H_2O$ + $SiO_2$ + $Mg^{2+}$ → Serpentine + magnetite + $H^+$ + $\mathbf{H_2}$ | $18-34$ days |
| Late | Enstatite + cpx + Fe-rich serpentine + $H_2O$ → Mg-rich serpentine + magnetite + calcic silicate + $\mathbf{H_2}$ | $34-70$ days |

**Table 4.** Stages of the serpentinsation reaction (Marcaillou et al., 2011)

(Deville & Prinzhofer, 2016; Vacquand et al., 2018). $H_2-CH_4$-rich gas seeps are typically characterised by mantle-like C and noble gas characteristics, as evidenced by measurements from several locations including the Zambales ophiolite, Phillipines and New Caledonia. Fluid communication within fracture networks and mixing between $N_2$-rich $H_2-CH_4$-rich end members is the most likely cause for $N_2-H_2-CH_4$-rich gas seeps (Abrajano et al., 1990; Deville & Prinzhofer, 2016). The flux of deep gas into a shallow aquifer isolated from direct equilibrium with the atmosphere and fractionation during subsequent degassing is suggested by Deville and Prinzhofer (2016) as the simplest explanation for observed $^{20}Ne$ and $^{36}Ar$ concentrations. A schematic diagram of the distribution of different gas seeps with an ophiolitic terrain is shown Figure 5A.

The timescale of subsurface gas migration is also dependent on parameters that control groundwater transport properties. Experimental work by Lamadrid et al. (2017) used synthetic fluid inclusions as micro-reactors in olivine crystals to monitor serpentinisation rates in-situ and at serpentinisation conditions (280°C). Serpentinisation rates were strongly influenced by aqueous fluid salinity, with evidence of reaction after 5 days decreasing from 50% to zero as aqueous fluid salinity of synthetic inclusions increased from 1−10 wt%. The time taken to observe the first evidence of reaction for salinity experiments at 10 wt% was 120 days, with the average rate of reaction being two orders of magnitude lower than experiments conducted with $1-3.5$ wt% salinity (Lamadrid et al., 2017). The results of Lamadrid et al. (2017) support those of Rouméjon and Cannat (2014), and indicate that the forward reaction requires continual influx of a lower salinity aqueous fluid (seawater) to dilute the serpentinisation fluid and allow serpentinisation of olivine to continue. Hydrogen migration and emission from surface seeps is dependent on the interplay between generative processes (e.g. serpentinisation) and destructive processes (e.g. microbial consumption). Important factors which influence the balance between generation and consumption include the water/rock ratio of migration or injected fluids (e.g. stimulated hydrogen generation, see next section), fluid chemistry and the formation of Fe(III)-bearing secondary phases (Templeton et al., 2024).

The results of Lamadrid et al. (2017) and Rouméjon and Cannat (2014) compliment experimental results of hydrogen dissolution by Iglauer et al. (2012) and Hosseini et al. (2022) (see earlier sections), and lead to an overall consensus that the salinity of the carrier fluid (i.e., groundwater) is a major controlling factor in both the amount of hydrogen gas generated and its rate of transport within sedimentary basins and ophiolitic terranes.

### Stimulated hydrogen generation

Over the last few years, the concept of stimulated geological hydrogen, also known as 'orange' hydrogen, has gained significant momentum (e.g., Osselin et al. (2022); Templeton et al. (2024)). Hydrogen generation may be stimulated by the injection fluids into target rock formations rich in reactive Fe(II)-bearing minerals to promote the overar-

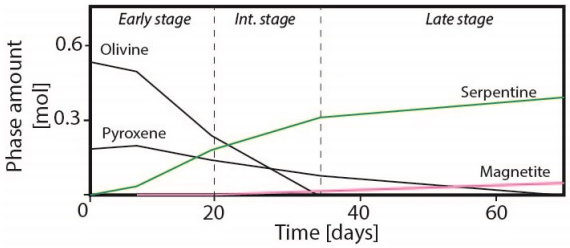


**Figure 4.** Evolution of mineral phases during serpentinisation reactions shown on Table 4. Serpentinisation products are shown in red (serpentinite) and red (magnetite). Magnetitie crystallises first and is responsible for $H_2$ generation during the early stage. During the intermediate phase, clinopyroxene is absent due to a lack of enrichment of calcium. During the late stage, olivine is no longer the reactive species and is replaced by serpentine formed during the early phase as the reactant. Late stage serpentine is Mg-rich and distinct from early stage serpentine. Modified from (Marcaillou et al., 2011).

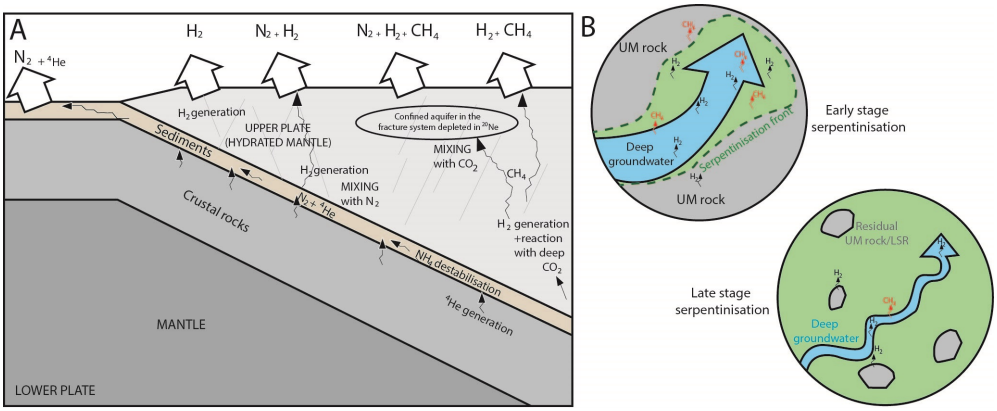


**Figure 5.** A = Conceptual diagram explaining gas compositions found at ophiolite-related seeps. B = Conceptual diagram showing progression of serpentinisation reaction and fluid migration pathways. UM rock = ultramafic rock. As serpentinisation of a rock volume progresses, water/rock ratios decrease significantly due to volume expansion and reduced permeability of serpentine (O'hanley, 1992). During late stage serpentinisation, $H_2$ generation decreases significantly due to reduced contact between serpentinisation fluids (e.g. deep groundwater) and reactants (unreacted ultramafic rock and early stage Fe-rich serpentine). Modified from (Marcaillou et al., 2011; Greenberger et al., 2015; Deville & Prinzhofer, 2016; Vacquand et al., 2018).

761 ching reaction of $2FeO(rock) + H_2O \rightarrow Fe_2O_3(rock) + H_2$. Most commonly, these are
762 found within ultramafic rocks or ophiolites. $H_2$ is then extracted by recirculating injected
763 fluids to the surface, if the required (bio) geochemical conditions for rapid hydrogen pro-
764 duction have been met (Templeton et al., 2024). Development of this relatively new con-
765 cept has been spurred by the recent U.S Department of Energy announcement of fund-
766 ing to support research into the production of geologic hydrogen through stimulated min-
767 eralogical processes (of Energy, 2024).

768 However, it is worth noting that the term 'orange' hydrogen has a broader mean-
769 ing within the literature, and includes chemical processes that break down traditional
770 hydrocarbons and biofuels (e.g., crude oil, natural gas, gasoline, biogas, etc.) into hy-
771 drogen with no carbon dioxide byproduct (Neelameggham et al., 2022). A notable re-
772 cent study that explores this includes the generation of $H_2$ from $H_2S$ by thermal split-
773 ting, a process which is potentially $\sim 38\%$ more economically viable than green hydro-
774 gen production (Nova et al., 2023). As this review is focussed on subsurface hydrogen
775 and migration, we do not explore industrial and chemical processes capable of produc-
776 ing hydrogen and avoid the term 'orange' hydrogen to prevent confusion with stimulated
777 hydrogen generation, i.e. due to the injection of fluids within subsurface geological for-
778 mations.

779 Osselin et al. (2022) assessed the reactive percolation of a $NaHCO_3$-rich brine at
780 160°C and 280°C in natural serpentinite cores in order to study the dynamic competi-
781 tion between serpentinisation and carbonation of ultramafic formations. Their results
782 are used to suggest that up to 100 trillion tonnes of $H_2$ could be produced from Fe(II)-
783 bearing rocks near Earth's surface. Similar to the serpentinisation reactions shown on
784 Table 3, the experiments of Osselin et al. (2022) were completed over a time period of
785 days. However, it is important to note that permeability reductions of several orders of
786 magnitude were observed and attributed to the precipitation of carbonates in the main
787 percolation paths. In mafic rocks, permeability is produced by fractures and the reduc-
788 tion in fracture permeability with time can be approximated by an exponential function:
789 $k_f = k_{f0}e^{-t/t^*}$, where $k_{f0}$ is the starting permeability of the modelled interval and $t^*$
790 is the characteristic decay time of the best fit exponential function in hours (Farough
791 et al., 2016). Precipitation of carbonates over silicates is favoured due to fast reaction
792 kinetics in comparission to flow rates. Osselin et al. (2022) conclude that the spatio-temporal
793 lengthscales associated with the different chemical reactions are directly linked to the
794 ratio of chemical reaction rate and transport (also known as the Damkokhler number)
795 and to the type of reaction regime (transport-limited vs reaction-limited). They inter-
796 pret their results as a dynamic interplay between dissolution and precipitation, controlled
797 by the local flow rate and the local pore geometry. Osselin et al. (2022) note that the
798 complex pore size distribution in natural rocks leads to very different behavior even for
799 a homogeneous mineralogy. Hence, the work of Osselin et al. (2022) demonstrates the
800 significance of changes in material properties of host rocks due to the flow of fluids used
801 to liberate hydrogen from mafic minerals, which will occur on a timescale of days.

802 More recently, Templeton et al. (2024) discusses factors that influence the timescales
803 of fluid migration through the Semail Ophiolite, Oman, such as the hydraulic conduc-
804 tivity of partially-hydrated peridotites, the extent of fracturing, and the geochemical dy-
805 namics of the subsurface environment. Fluid flow in the most shallow and fissured rocks
806 occurs in transmissive zones located within 50 m of the surface, indicating that fluid dy-
807 namics are highly heterogeneous. Templeton et al. (2024) also describes that some zones
808 are most sensitive to conductive channels, such as partially mineralised fractures, whereas
809 other zones are supplied from rocks above and below. This complexity, including the pres-
810 ence of fractures partially filled with secondary minerals produced from both modern and
811 ancient water/rock reactions, suggests that fluid migration rates and, by extension, hy-
812 drogen migration rates through the crust are highly variable and dependent on local ge-
813 ological conditions. In contrast to Osselin et al. (2022), the analyses of Templeton et al.

(2024) were conducted at low temperature (25°C), demonstrating that the sensitivity of fluid flowpaths are not restricted to high-temperature systems only or within deeper parts of geological basins.

### Adsorption

The migration of hydrogen may be prevented by the physical adsorption of $H_2$ molecules to the surface of minerals, particularly clays. This is demonstrated by Truche et al. (2018), who demonstrate hydrogen enrichment of $< 500$ ppm (0.25 mol/kg of rock) within organic-poor ($< 0.5$ wt % total organic carbon) clays composed of illite, chlorite and kaolinite from the Cigar Lake uranium ore deposit, Canada. Furthermore, recent experiments by L. Wang, Cheng, et al. (2023) demonstrate that hydrogen adsorption is significantly influenced by the pore structure and specific surface area of the clay minerals, with a notable increase in hydrogen adsorption capacity under high pressure and a decrease at higher temperatures, independent of the clay mineral type. L. Wang, Cheng, et al. (2023) show that whilst montmorillonite and chlorite only adsorb hydrogen on their external surface, palygorskite and sepiolite can adsorb hydrogen on both the bulk phase and the external surface. However, adsorption capacity may be compromised by a range of factors, including the presence of water and other adsorbed gases (e.g., $CO_2$, $CH_4$, He) which may compete for adsorption sites.

Whilst significant volumes of hydrogen may accumulate within clay-rich rocks due to adsorption, the degree to which this affects overall hydrogen migration on the basin-scale is, however, an open question. Truche et al. (2018) estimate that $4 - 17\%$ of $H_2$ produced by water radiolysis over the 1.4 Ga lifetime of the Cigar Lake uranium ore deposit is trapped in the surrounding clay alteration halos, thus leaving $83-96\%$ hydrogen unaccounted for. Despite adsorption, hydrogen will migrate due to advection along fractures and by diffusion, with breakthrough times varying on the scale of years per metre for most rocks, including clays (Table 2). Hence, it is reasonable to assume the timescale over which adsorption sites become occupied must be fairly rapid and on the scale of years to thousands of years for volumes of clay-rich rocks typically within sedimentary basins. In reality, it is likely that whilst adsorption may trap significant and potentially economic volumes of hydrogen within clay-rich rocks and remain stable over geological timescales, the majority of hydrogen within sedimentary basins remains transient and mobile.

### *Microbes*

Microbial reactions within host rocks and sediments are important moderators of hydrogen flow in the subsurface. Microbial activity may lead to both the generation and loss of hydrogen as it migrates through a reservoir, as summarised on Table 5. Microbial reactions are dependent on many factors, such as environment (e.g., pH, salinity), iron ($Fe^{3+}$) content of host rocks, groundwater recharge and the presence of other reduced gases from deeper in Earth (Anderson et al., 1998; Stevens & McKinley, 2000). There is a growing consensus that subsurface microbial communities are independent of photosynthesis for carbon and hydrogen supply, and are primarily or completely dependent on abiotc hydrogen sources in various geological settings as an energy source (Kotelnikova & Pedersen, 1998; Takai et al., 2004; L. H. Lin et al., 2005; McCollom & Amend, 2005; Nealson et al., 2005; Escudero et al., 2018; Gregory et al., 2019). These microorganisms consist of Bacteria and Archaea and exist in great abundances within the subsurface, with $\sim 10^4 - 10^8$ cells/gram of rock up to several km deep and $\sim 2 - 6 \times 10^{29}$ cells within the continental subsurface (Dutta et al., 2018; Magnabosco et al., 2018). For microbial life to survive, temperature limits must lie between $-15$°C to $+121$°C, corresponding to depths of up to $3.5 - 4.5$ km beneath Earth's surface at normal geothermal gradients of $30\pm5$°C/km. Temperature, pressure and salinity are important factors for the prevalence of single-celled microorganisms within the subsurface that are responsible for using hydrogen in their metabolism. Whilst there is little to no information about pres-

sure or brine salinity thresholds, neutral pH ($pH = 6 - 7$) conditions generally correspond to the greatest abundance and diversity of microbial life. However, microbial life may exist within the pH range $0 - 11$ (Dopffel et al., 2021).

In terms of migration, literature on the impact of microbial reactions on hydrogen is scant, with the overwhelming majority of recent and legacy research focused on assessing microbial hydrogen generation, consumption and associated environmental risk (e.g. $H_2S$ generation). As generative and destructive processes alter the amount of hydrogen within a subsurface system, it is conceptually reasonable to consider their role in migration as a moderator of hydrogen flow, whereby the rate of hydrogen transport through a medium influenced by microbes will depend on the kinetics and rates of microbial-hydrogen reactions. Thus, microbial reactions represent an important sink in the migration pathway of hydrogen from depth to the surface. Harris et al. (2007) present one of the few experimental assessments of microbial community metabolism directly within a groundwater environment, and estimate hydrogen consumption rates in-situ injection/withdrawal tests conducted in two geochemically varying, contaminated aquifers. The results of Harris et al. (2007) show that first-order hydrogen consumption rates varied from 0.002 nM $h^{-1}$ for an uncontaminated, aerobic site to 2.5 nM $h^{-1}$ for a contaminated site where sulphate reduction was a predominant process. Notably, the hydrogen consumption rate reduced to zero within a denitrifying zone and in the presence of air or an antibiotic mixture, thus highlighting potential sensitivity to environmental perturbations on field microbial activities on the timescale of several hours (Harris et al., 2007). These results may be interpreted as meaning the degree to which subsurface microbial activity moderates hydrogen flow may vary on timescales relevant to groundwater flow through the host rock or sediment, e.g. the acidity and salinity of pore fluids in top soils may vary on timescales of hours - days, whereas deeper rocks and aquifers may attenuate environmental signals over thousands of years or longer. Interestingly, Templeton et al. (2024) demonstrate that the alteration of the chemical composition of fluids introduced into geological formations during stimulated hydrogen generation is pivotal for the optimal generation of Fe(III)-enriched secondary mineral phases. Templeton et al. (2024) argue that modifications in fluid chemistry should be strategically engineered to concurrently diminish the microbial uptake of $H_2$ within the stimulated region, whilst maintaining elevated capacities for biogenic hydrogen assimilation in the shallow groundwater systems. The assimilation of biogenic hydrogen into shallow groundwater is essential as this will be saturated with oxidising agents such as nitrate, sulfate, and dissolved inorganic carbon. The recommendations of Templeton et al. (2024) serves to mitigate the risk of unintentional hydrogen emissions into the atmosphere, where it contributes as an indirect greenhouse gas

The ability of host rocks to sustain microbial activity on geological timescales may also be dependent on whether the rocks contain sufficient reduced iron and other dependent nutrients (Gregory et al., 2019). The compilation of experimental results by Roden and Jin (2011) show that the relationship between microbial yield and the free energy of aerobic and anaerobic metabolism of hydrogen in soils and sediments follow the same linear trend as other compounds, such as glucose, ethanol, formate, acetate, lactate, propionate, butyrate. Roden and Jin (2011)'s results indicate that it is possible to estimate microbial yield values within a factor of 2 (i.e. error = $\pm 100\%$) using a simple linear relationship, although it should be noted that errors are greatest for hydrogen metabolism. The results of Harris et al. (2007) and Roden and Jin (2011) indicate that it may be possible to quantify the role played by subsurface microbial activity as a moderator of hydrogen transport, however further research is required in this area to determine the relationship between subsurface environmental change and the timescale of hydrogen migration.

| Process | Reaction | $\Delta G^{0'}$ kj mol$^{-1}$ $H_2$ | Reference |
|---|---|---|---|
| **Microbial hydrogen generation** | | | |
| Fermentation | Multiple pathways that breakdown large organics into smaller organics, e.g., mixed acid fermentation e.g., $C_6H_{12}O_6 + 4H_2O \rightarrow 2CH_3COO_3^- + 2HCO_3^- + 4H^+ + 4H_2$ | $-54.0 - 24.2$ | (Thauer et al., 1977; Conrad, 1999) (Schink et al., 2002; Gregory et al., 2019) |
| Nitrogen fixation (nitrogenase activity) | $N_2 + 8H+ + 8e^-$ ($Fd_{red}$) $\rightarrow 2NH_3 + H_2$ ($+Fd_{ox}$) | $-18.1$ | (Thauer et al., 1977; Conrad, 1999) (Schink et al., 2002; Gregory et al., 2019) |
| Anaerobic carbon monoxide oxidation | $CO + H_2O \rightarrow CO_2 + H_2$ | $-19.9$ | (Thauer et al., 1977; Conrad, 1999) (Schink et al., 2002; Gregory et al., 2019) |
| Phosphite oxidation | $H_3PO_3 + H_2O \rightarrow H_3PO_4 + H_2$ | $-46.3$ | (Thauer et al., 1977; Conrad, 1999) (Schink et al., 2002; Gregory et al., 2019) |
| Acetate oxidation | $\frac{1}{4}CH3COO^- + 14\ H^+ + \frac{1}{2}H_2O \rightarrow H_2 + \frac{1}{2}\ CO_2$ | 23.7 | (Thauer et al., 1977; Conrad, 1999) (Schink et al., 2002; Gregory et al., 2019) |
| **Microbial hydrogen consumption** | | | |
| Hydrogenotrophic methanogenesis | $HCO3^- + H_2 + \frac{1}{4}H^+ \rightarrow \frac{1}{4}CH_4 + \frac{3}{4}H_2O$ | $-33.9$ | (Schink et al., 2002; Greening et al., 2016) (Gregory et al., 2019; Dopffel et al., 2021) |
| Acetogenesis | $\frac{1}{2}HCO_3^- + H_2 + \frac{1}{4}H^+ \rightarrow \frac{1}{4}CH_3COO^- + 2H_2O$ | $-26.1$ | (Schink et al., 2002; Greening et al., 2016) (Gregory et al., 2019; Dopffel et al., 2021) |
| Sulphate reduction | $\frac{1}{4}SO_4^{2-} + H_2 + \frac{1}{4}H^+ \rightarrow \frac{1}{4}HS^- + H_2O$ | $-38.0$ | (Schink et al., 2002; Greening et al., 2016) (Gregory et al., 2019; Dopffel et al., 2021) |
| Sulphur reduction | $H_2 + S \rightarrow H_2S$ | $-33.1$ | (Schink et al., 2002; Greening et al., 2016) (Gregory et al., 2019; Dopffel et al., 2021) |
| Iron(III) reduction | $2FeOOH + H_2 + 4H^+ \rightarrow 2Fe^{2+} + 4H_2O$ | $-228.3$ | (Schink et al., 2002; Greening et al., 2016) (Gregory et al., 2019; Dopffel et al., 2021) |
| Aerobic hydrogen oxidation | $H_2 + \frac{1}{2}O_2 \rightarrow H_2O$ | $-237$ | (Schink et al., 2002; Greening et al., 2016) (Gregory et al., 2019; Dopffel et al., 2021) |
| Dehalorespiration | Halogenated compounds + $H_2 \rightarrow$ dehalogenated compounds + 2HCl | $-230$ to $-187$ | (Schink et al., 2002; Greening et al., 2016) (Gregory et al., 2019; Dopffel et al., 2021) |
| Fumarate respiration | $H_2$ + fumarate $\rightarrow$ succinate | $-86.2$ | (Schink et al., 2002; Greening et al., 2016) (Gregory et al., 2019; Dopffel et al., 2021) |
| Denitrification | $\frac{2}{5}NO3^{-1} + H_2 + \frac{2}{5}H^+ \rightarrow \frac{1}{5}N2 + \frac{6}{5}H_2O$ | $-240.1$ | (Schink et al., 2002; Greening et al., 2016) (Gregory et al., 2019; Dopffel et al., 2021) |

**Table 5.** Examples of microbial hydrogen generating and consuming reactions. Compiled from (Schink et al., 2002; Greening et al., 2016; Gregory et al., 2019; Dopffel et al., 2021).

## Diffusion versus advection

A property that distinguishes hydrogen from other fluids within geological basins is its ability to migrate through rocks occurs via diffusion or advective processes from human to geological timescales. In reality, it is reasonable to assume that hydrogen flow-paths will be a function of both diffusive and advective processes (e.g., Figure 7) and overall fluid chemistry. However, the ability to predict the behaviour of hydrogen in the subsurface similar to other fluids, such as hydrocarbons and groundwater, remains largely unresolved. The results of Mathiesen et al. (2023); Hutchinson et al. (2024) indicate that pore throat diameter, and therefore capillary entry pressure, exert a primary control on the mode of hydrogen migration, with increasing advective dominance at larger pore throat sizes (i.e. sandstones) and increasing diffusive dominance at smaller pore throat sizes (i.e. shales, evaporites). Lodhia and Clark (2022) approximate hydrogen mobility and buoyancy by solving the Darcy flow equation using a series of steps and use lithological parameters representative of general rock types. Their method may be applied to estimate the basin-scale maximum vertical velocity, $v_{max}$, of pure advective $H_2$ gas-flow as the product of mobility and buoyancy, as it accounts for upscaling (due to macro-scale features such as faults and fractures), geological regime (e.g., normal, overpressured or hydrostatic) and geothermal gradient (Lodhia, 2023). However, there is no clear relationship between $v_{max}$, permeability and porosity (Lodhia & Peeters, 2024). The transition between diffusive and advective flow for pure and multiphase $H_2$, known as the trans-slip flow boundary, may be calculated using a charecteristic Knudsen number value of 0.1 (Hutchinson et al., 2024; Sakhaee-Pour & Alessa, 2022; Roy et al., 2003). We apply data from Strauch et al. (2023) and Fick's first law to calculate diffusion velocities, $v_{diff}$, for dry and wetted sandstone, evaporties and clay. Due to a lack of data in the literature, $v_{diff}$ is not calculated for hydrogen migration in carbonates. Calculated basin-scale $v_{max}$ and $v_{diff}$ values are shown on Figure 6A−B and indicate diffusive velocities are several orders of magnitude smaller than advective velocites and that $v_{max}$ decreases exponentially with increasing clay content across all rock types. Advective flow of $H_2$ becomes less effective at shallow depths ($< 400$ m) due to the rapid increase in mean free paths. Under multiphase subsurface conditions, advective flow will be impaired due to water occupying and restricting pore space, causing the diffusion-advection boundary to be displaced to larger pore throat sizes (Hutchinson et al., 2024). It is also reasonable to assume that diffusion velocities for hydrogen in carbonates will follow a similar trend to other rock types and be several orders of magnitude smaller than $v_{max}$ values. Hence, calculations of $v_{max}$, $v_{diff}$ and the position of the diffusion-advection boundary provide an estimate for the timescale and mode of hydrogen migration at different depths in shallow sedimentary basins for a range of rock types. We hypothesise that hydrogen migration is dominated by diffusion at shallow depths and operates on a timescale of $<$ 0.5 cm year$-1$ for clastic rocks, shale, evaporites and probably carbonates, which decrease by an order of magnitude for water-saturated rocks or sediments. At intermediate depths, the boundary between diffusive and advective flow marks a peak in migration velocity on the timescale of $> 0.1$ and $< 10$ m year$^{-1}$ for most clastic and carbonate rocks, with the exception of dolomites which have advective velocities from $\sim 100-1000$ m year$^{-1}$. The boundary between diffusive and advective hydrogen flow is not uniform across different rock types, such that multiphase conditions cause displacement towards more coarsely grained rocks and an increased depth envelope for diffusive migration. Advective velocities decrease with depth due to the reduction in pore throat sizes and corresponding increase in capillary entry pressures required for hydrogen flow. Furthermore, whilst increased clay content will affect the timescale of advective flow, the effect on diffusion is minimal.

Future experimental research should focus on improving understanding of porosity and water saturation relationships relevant for hydrogen, as due to a lack of data in the literature, Lodhia and Clark (2022) apply estimates of oil-water and gas-water sys-

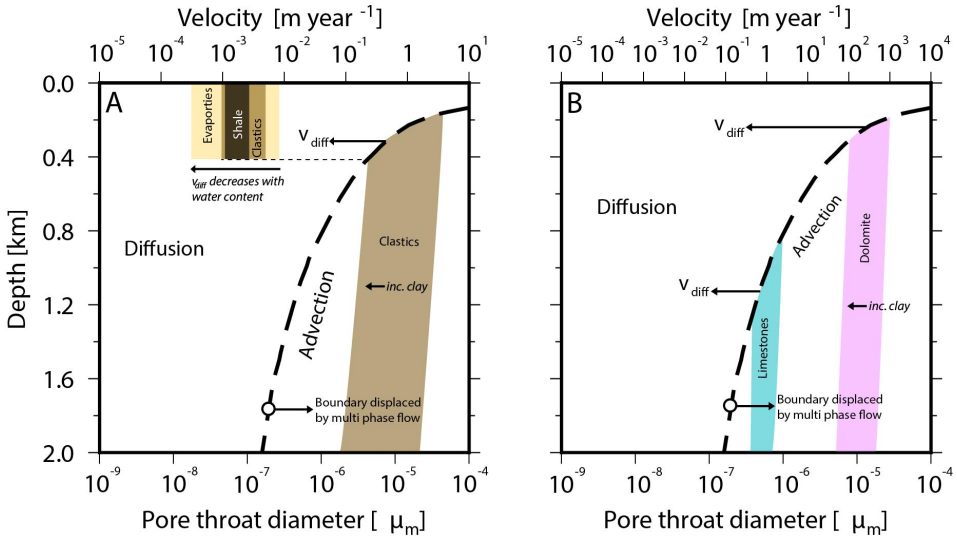


**Figure 6.** Maximum vertical velocity ($v_{max}$) and diffusion velocity ($v_{diff}$) calculated for various rock types using the method of Lodhia and Clark (2022) and data from Hantschel and Kauerauf (2009) and Strauch et al. (2023), respectively. A = velocity $v_{max}$ and $v_{diff}$ for clastic rocks. Dashed horizontal line indicates the maximum depth of transition between advective and diffusive migration for pure $H_2$. $v_{diff}$ decreases with increasing water content due to a rapid increase in mean free paths (i.e., increased collisions between $H_2$ and water molecules) whilst $v_{max}$ decreases with increasing clay content due to increased capillary entry pressure associated with decreasing pore throat diameter (e.g. Hutchinson et al. (2024)). B = $v_{max}$ for carbonate rocks. We do not calculate $v_{diff}$ values for carbonates due to a lack of data within the literature, however assume these to follow a similar trend to clastic rocks and be several orders of magnitude smaller than corresponding $v_{max}$ values (see labelled arrows). Curved dashed line = diffusion-advection boundary for pure $H_2$ calculated using a Knudsen number of 0.1 (Hutchinson et al., 2024). This boundary is displaced to larger pore throat sizes for multiphase subsurface flow as indicated by circled arrows.

tems. Future experimental studies may also focus on testing both the robustness of Lodhia and Clark (2022)'s approximations and our hypotheses.

## Discussion

The migration of hydrogen through the subsurface is a topic seldom addressed directly, yet is critical for exploration and geological storage investigations. To understand the dynamics of the subsurface hydrogen cycle within sedimentary basins and Earth's surface, we must take a holistic view of its supply, emission and intermediate processes.

Within geological basins, long-term hydrogen supply from the radiolysis of water within crystalline basement, Archean - Proterozoic cratonic rocks and other hydrogen abundant mafic igenous rocks will remain steady over geological timescales. However, hydrogen migration pathways will be disproportionately affected by specific processes operating within small regions within sedimentary basins and Earth's crust, such as microbial reactions in soil or regolith, advection of fluids along faults and 'trapping' on timescales relative to humans by wet or evaporitic sediments. Environmental factors, such as salinity and temperature may change the dynamics of subsurface hydrogen systems rapidly, for example a saline aquifer changing from a barrier to a carrier due to an influx of fresh meteoric water following heavy rainfall. Hydrogen supply rates within generative systems will be primarily controlled by the availability of fresh water, such as rainfall on ophiolitic systems or groundwater contact with buried igenous rocks.

The rate of diffusive migration of hydrogen from crystalline rocks into surrounding sediments will operate on timescales of $1-1000$ years (Figure 2), and be controlled primarily by grain size and temperature. Experimental results from the literature indicate that native hydrogen entrained within the mineral structure of crystalline rocks within the shallow Earth may diffuse on geological timescales from the most common rock forming minerals. Geochemical data obtained by Parnell and Blamey (2017) indicate that common felsic lithologies, such as granites, gneiss and conglomerates of Archean - Proterozoic ($> 1600$ Ma) age consistently contain an order of magnitude greater hydrogen in their entrained fluid than very young ($< 200$ Ma) granites. Parnell and Blamey (2017) found that sedimentary rocks containing clasts of old basement also included a greater proportion of hydrogen than young granites and hypothesise that a signature of hydrogen in the basement could be conferred to the sediment and that modern sediment derived from old and young basement retains the signature of more or less hydrogen, respectively (Figure 7). It should be noted however that the experimental results summarised by Parnell and Blamey (2017) refer to bulk lithologies whereas those of Farver (2010) refer to individual minerals (e.g. olivine and quartz). Furthermore, the preservation of high hydrogen abundances within fluid inclusions and mineralised veins in ancient granites has been observed (Bourdet et al., 2023). Hence, diffusion from enriched Archean - Proterozoic crystalline basement and their derived sedimentary products, e.g., conglomerates, may supply a 'background' hydrogen flux to overlying sedimentary basin rocks on geological timescales. This is consistent with the widely documented observation of higher hydrogen fluxes in sedimentary basins in continental cratonic regions underlain by Archean - Proterozoic basement (e.g. Zgonnik (2020); ? (?)). In the case of rapidly cooled upper mantle rocks, e.g. MORBs, volcanic glasses, pillow lavas, however, grain sizes may be many orders of magnitude smaller than their continental counterparts and within the nanometre scale (e.g., Schlinger et al. (1988)). Hence, hydrogen diffusivity in rapidly cooled crystalline rocks and at MOR settings will be significantly faster than in continental settings and potentially only a few orders of magnitude slower than the lower temperature ranges of diffusivity experiments, i.e. 100 Ka - Ma or faster. This is significant, since the age of most oceanic crustal rocks is $< 60$ Ma (Seton et al., 2020), hydrogen diffusion within oceanic crustal rocks will operate on the same timescale as the age of rocks themselves and provide a mechanism for the degassing of mantle hydrogen to the surface and oceans. Figure 7 summarises the characteristic migration timescales

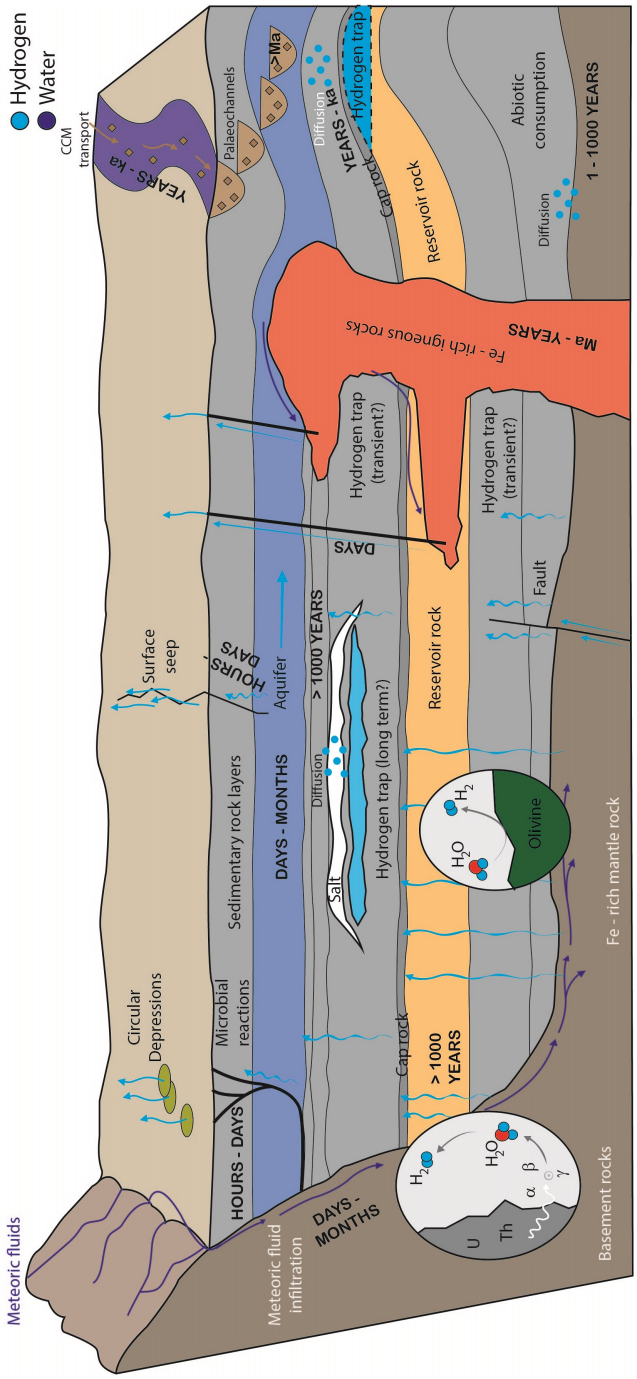


**Figure 7.** Conceptual method for modelling workflow, migration and indicative timescales through sedimentary basins. Blue arrows indicate advective transport of hydrogen. Fe-rich lithologies (e.g. granites) characterise Archean - Proterozoic continental crystalline basement within cratonic regions and igneous intrusive rocks. Diffusion through geological barriers to hydrogen migration, e.g. salt and igneous intrusions may limit hydrogen migration by thousands to millions of years, depending on mineralogy and lithology (Farver, 2010; Parnell & Blamey, 2017). Continental clastic material (CCM) derived from terrains enriched in hydrogen (e.g. Archean - Proterozoic basement) is believed to be responsible for the provenance of high hydrogen concentrations in some sedimentary basin rocks (Parnell & Blamey, 2017). The transport of CCM (brown diamonds and arrows) by fluvial systems and accumulation in palaeochannel deposits is shown for conceptual purposes. Modified from Hand (2023)

for hydrogen transport through different parts of a sedimentary basin as described in this article.

Whilst faulting and fluid flow have been extensively reviewed in the literature, their impact on hydrogen migration have only recently gained significant attention. Observations of hydrogen pulses prior to seismic activity are not well documented, but can be analogous to increased $CO_2$ emissions possibly due to enhanced porosity of the soil due to faulting, and accelerated water rock interactions and soil gas emission within the fault zone (e.g., Z. Liu et al. (2023)). Early work by by Wakita et al. (1980) hypothesised the production of hydrogen by fault movement, based on measurements of elevated hydrogen concentrations ($> 3\%$ by volume) around active fault zones in southwestern Japan compared to background measurements of $\sim 0.5$ ppm. Su et al. (1992) identified the potential reduction in strength of crystalline minerals (e.g., calcite, dolomite, antigorite) due to hydrogen infiltration at low pressures, leading to the weakening of rocks and initiation of faulting. Hydrogen gas measurements and particle size distribution analyses by Niwa et al. (2011) within an active fault zone indicate that hydrogen gas mostly migrated in permeable fracture zones by advection with groundwater. Firstov and Shirokov (2005) measured seven pulses of hydrogen discharge against background levels in a fault zone trending parallel the Kuril - Kamchatka geostructural zone, Russia, from 1999−2003. Hydrogen pulses preceding seismic events lasted from 1.5−6 hours and were 2−14 times higher than measured background levels. Firstov and Shirokov (2005) found that $< 80\%$ earthquakes with $M_W \geq 5.6$ in the southern Kamchatka region occurred within one month of measured hydrogen pulses and considered such events as short-term earthquake precursors. In recent years, the migration of natural hydrogen from deep crustal sources along kilometre-scale faults which penetrate crystalline basement have been recorded in several locations across the world (e.g., Brazil, France, Mali) (Prinzhofer et al., 2018; Deronzier & Giouse, 2020; Donzé et al., 2020; Rezaee, 2021; Frery, Langhi, et al., 2021; Lefeuvre et al., 2021, 2022).

### Recent hydrogen discoveries and possible importance to migration pathways

Following the landmark discovery of natural hydrogen at Bourakebougou in Mali by Prinzhofer et al. (2018), subsequent research has uncovered numerous hydrogen deposits worldwide. In this section, we review several recent discoveries and examine potential relationships between gas composition and fluid migration pathways.

A regional geochemistry study by Lévy et al. (2023) in Albania and Kosovo focused on natural springs, revealing a site in northern Kosovo with a hydrogen concentration of 16%, pointing to serpentinisation of peridotites as a hydrogen source. Notably, this study found no correlation between hydrogen and helium concentrations but did observe substantial organic and crustal contributions ($CH_4$ and $N_2$). Contrastingly, recent data from South Australia and direct measurements from the Bulqizë chromite mine in Albania report significant hydrogen outgassing, with $H_2$ concentrations $> 80\%$ and varying but minor $N_2$, $CO_2$ and $CH_4$ components (Goh, 2023; Hydrogen, 2023; Truche et al., 2024; Yeo, 2023). Interestingly, whilst the results of Lévy et al. (2023) indicated no a clear connection between hydrogen and helium in the context of serpentinisation, Karolytė et al. (2022) documented He-rich hydrocarbon gases in South Africa's Witwatersrand Basin, where the scarcity of mafic and ultramafic minerals capable of serpentinisation suggests radiolytic hydrogen production as the predominant mechanism. Despite the detection of hydrogen alongside $CH_4$ and $N_2$ in both scenarios, the system described by Karolytė et al. (2022) is not associated with hydrocarbon source rocks. Transportation over vast distances and a significant degree of interaction with groundwater dilute He and lower H/He ratios (Ballentine & Lollar, 2002; Gilfillan et al., 2008). Hence, observed He concentrations in the Witwatersand Basin by Karolytė et al. (2022) may be explained by

long periods of quiescence for He accumulation within a closed system, characterised by its hydrogeological systems being isolated and He preservation.

These examples highlight the rapid conversion of hydrogen to methane in surface environments and the influence of gas composition on migration pathways, particularly the impact of helium content on gas mixture compositions over geological timeframes. Prinzhofer and Cacas-Stentz (2023) present theoretical analyses suggesting that advective leakage of hydrogen-bearing gases out of subsurface reservoirs affects their overall composition, leading to an increase in nitrogen and methane content at the expense of hydrogen. Their findings suggest a dichotomy where hydrogen, though renewable on human scales, is diluted on geological timescales, while helium, due to its inert nature, accumulates over similar periods. Their models demonstrate the rapid formation of natural hydrogen deposits, with instances of H2-dominant gas accumulations $\sim$ 500 years old in Mali, evolving to CH4-dominant mixtures $\sim$ 40 ka old in Turkey, and $N_2$-rich variants within timescales of millions of years, exemplified by the Amadeus Basin in Australia (Boreham et al., 2021).

These analyses indicate that $H_2$-rich gas subsurface accumulations are dependent on recent or ongoing hydrogen generation, whilst fossil accumulations are characterised by lower $H_2$ abundances and greater organic and crustal component abundancies. The relationship between fluid migration and helium is paradoxical, given that for high He concentrations to be preserved alongside high H2 concentrations (e.g. Hydrogen (2023), migration must be rapid enough to prevent dilution whilst the isolation of fluids over billions of years could allow He to accumulate whilst $H_2$ is lost (e.g. Karolytė et al. (2022)). The relationship between surface gas seep compositions and migration pathways is more nuanced, given that microbial methanogenesis (Table 5) is depth-dependent (e.g., Truche et al. (2024)). Hydrogen consumption within the shallowest levels of the subsurface ($<$ 1 m) may imprint a diurnal variation onto otherwise long-lived high-concentration ($>$ 50%) $H_2$ signals (e.g. Myagkiy, Moretti, and Brunet (2020)). For high $H_2$ concentrations to be preserved to the surface, we hypothesise that fluid migration pathways operate on both short timescales and lengthscales such that the opportunity for environmental hydrogen uptake is severely limited. However, we propose that seeps characterised by low hydrogen concentrations ($< 20\%$, e.g. Lévy et al. (2023)) typify migration pathways over greater distances and timescales, such as basin-scale transport along faults and fractures, whereby substantial amounts of hydrogen are lost due to microbial consumption and other processes.

## Conclusion

Hydrogen within the subsurface remains elusive. While entrenched into Earth during planetary formation, the exchange of hydrogen between materials is prevalent during subsurface processes at all depths. Significant advances in understanding the distribution and generation of natural hydrogen have been made in recent literature, however large gaps remain in our understanding of large-scale hydrogen migration. The timescale of hydrogen migration throughout Earth varies from billions of years to days, and is dependent on a wide range of lithological and environmental factors. Grain size, temperature and fluid salinity exert important controls on hydrogen diffusivity in crystalline and sedimentary rocks. Diffusive and advective migration of hydrogen vary by several orders of magnitude, however operate on timescales of $<$ 0.5 cm to m per $>$ 1000 m per year, respectively. Fluid migration along faults and fractures is controlled by rock properties, subsurface stress regimes and groundwater properties. The phenomena of gas-induced fault opening and hydrogen pulses associated with seismic activity require further research. Microbial reactions moderate subsurface hydrogen flow by altering mass balance on differing timescales related to depth and environmental factors. Understanding the transition between diffusive and advective flow of hydrogen and multiphase fluids within different rock types in the subsurface remains a key challenge.

## Acknowledgments

This work was supported by the Impossible Without You program, Hydrogen Energy Systems Future Science Platform and Hydrogen Industry Mission, CSIRO. The authors would like to thank Trevor Rapson for his initial suggestion to write this review. We thank Axel Suckow and Joel Sarout for reviewing this manuscript. Thanks are also given to Kate Holland for her support of this project and to our colleagues and associates for their discussions.

## Data availability statement

The authors confirm that the data supporting the findings of this study are available within the article. Code used to calculate fluid properties (Figure 6) using the method of Lodhia and Clark (2022) is published at `https://github.com/lodhia92/hydrogen_mobility` (Lodhia, 2023).

## Declarations

The authors declare no conflicts of interest.

## References

Abrajano, T. A., Sturchio, N. C., Bohlke, J. K., Lyon, G. L., Poreda, R. J., & Stevens, C. M. (1988). Methane-hydrogen gas seeps, zambales phiolite, philippines: Deep or shallow origin? *Chemical Geology*, *71*, 211-222.

Abrajano, T. A., Sturchio, N. C., Kennedy, B. M., Lyon, G. L., Muehlenbachs, K., & Bohlke, J. K. (1990). *Geochemistry of reduced gas related to serpentinization of the zambales ophiolite, philippines* (Vol. 5).

Allègre, C., Staudacher, T., & P., M. S., Kurz. (1983). Constraints on evolution of earth's mantle from rare gas systematics. *Nature*, *303*, 762-766. doi: https://doi.org/10.1038/303762a0

Allègre, C. J., Moreira, M., & Staudacher, T. (1995). 4he/$^{3}$he dispersion and mantle convection. *Geophysical Research Letters*, *22*, 2325-2328. doi: 10.1029/95GL02307

Al-Yaseri, A., Yekeen, N., Mahmoud, M., Kakati, A., Xie, Q., & Giwelli, A. (2022). Thermodynamic characterization of h2-brine-shale wettability: Implications for hydrogen storage at subsurface. *International Journal of Hydrogen Energy*, *47*, 22510-22521. doi: 10.1016/j.ijhydene.2022.05.086

Anderson, R. T., Chapelle, F. H., & Lovley, D. R. (1998). Evidence against hydrogen-based microbial ecosystems in basalt aquifers. *Science*, *281*, 976-977. doi: 10.1126/science.281.5379.976

Andresen, K. J., & Huuse, M. (2011). 'bulls-eye' pockmarks and polygonal faulting in the lower congo basin: Relative timing and implications for fluid expulsion during shallow burial. *Marine Geology*, *279*, 111-127. doi: 10.1016/j.margeo.2010.10.016

Bagreev, A., Menendez, J. A., Dukhno, I., Tarasenko, Y., & Bandosz, T. J. (2004). Bituminous coal-based activated carbons modified with nitrogen as adsorbents of hydrogen sulfide. *Carbon*, *42*, 469-476. doi: 10.1016/j.carbon.2003.10.042

Ballentine, C. J., & Lollar, B. S. (2002). *Regional groundwater focusing of nitrogen and noble gases into the hugoton-panhandle giant gas field, usa.*

Bania, T. M., Rood, R. T., & Balser, D. S. (2002). The cosmological density of baryons from observations of 3 he + in the milky way. *Nature*, *415*, 54-57. doi: https://doi.org/10.1038/415054a

Berta, M., Dethlefsen, F., Ebert, M., Schäfer, D., & Dahmke, A. (2018). Geochemical effects of millimolar hydrogen concentrations in groundwater: An exper-

imental study in the context of subsurface hydrogen storage. *Environmental Science and Technology*, *52*, 4937-4949. doi: 10.1021/acs.est.7b05467

Bodnar, R. J., Azbej, T., Becker, S. P., Cannatelli, C., Fall, A., & Severs, M. J. (2013). Whole earth geohydrologic cycle, from the clouds to the core: The distribution of water in the dynamic earth system. *Special Paper of the Geological Society of America*, *500*, 431-461. doi: 10.1130/2013.2500(13)

Boreham, C. J., Edwards, D. S., Czado, K., Rollet, N., Wang, L., van der Wielen, S., ... Henson, P. A. (2021). Hydrogen in australian natural gas: occurrences, sources and resources. *The APPEA Journal*, *61*, 163. doi: 10.1071/aj20044

Boreham, C. J., Edwards, D. S., Feitz, A. J., Murray, A. P., Mahlstedt, N., & Horsfield, B. (2023). Modelling of hydrogen gas generation from overmature organic matter in the cooper basin, australia. *The APPEA Journal*, *63*, S351-S356. doi: 10.1071/aj22084

Boschi, L., Becker, T. W., & Steinberger, B. (2007). Mantle plumes: Dynamic models and seismic images. *Geochemistry, Geophysics, Geosystems*, *8*. doi: 10.1029/2007GC001733

Bouhifd, M. A., Jephcoat, A. P., Heber, V. S., & Kelley, S. P. (2013). Helium in earth's early core. *Nature Geoscience*, *6*, 982-986. doi: 10.1038/ngeo1959

Bourdet, J., Piane, C. D., Wilske, C., Mallants, D., Suckow, A., Questiaux, D., ... Aleshin, M. (2023). Natural hydrogen in low temperature geofluids in a precambrian granite, south australia. implications for hydrogen generation and movement in the upper crust. *Chemical Geology*, *638*, 1-18. doi: https://doi.org/10.1016/j.chemgeo.2023.121698

Burnside, N. M., Shipton, Z. K., Dockrill, B., & Ellam, R. M. (2013). Man-made versus natural co2 leakage: A 400 k.y. history of an analogue for engineered geological storage of co2. *Geology*, *41*, 471-474. doi: 10.1130/G33738.1

Capitanio, F. A., Nebel, O., Cawood, P. A., Weinberg, R. F., & Chowdhury, P. (2019). Reconciling thermal regimes and tectonics of the early earth. *Geology*, *47*, 923-927. doi: 10.1130/G46239.1

Capitanio, F. A., Nebel, O., Moyen, J. F., & Cawood, P. A. (2022). Craton formation in early earth mantle convection regimes. *Journal of Geophysical Research: Solid Earth*, *127*. doi: 10.1029/2021JB023911

Cartwright, J. (2011). *Diagenetically induced shear failure of fine-grained sediments and the development of polygonal fault systems* (Vol. 28). doi: 10.1016/j.marpetgeo.2011.06.004

Cartwright, J., James, D., & Bolton, A. (2003). The genesis of polygonal fault systems: A review. *Geological Society Special Publication*, *216*, 223-234. doi: 10.1144/GSL.SP.2003.216.01.15

Chabab, S., Kerkache, H., Bouchkira, I., Poulain, M., Baudouin, O., Édouard Moine, ... Cézac, P. (2024). Solubility of h2 in water and nacl brine under subsurface storage conditions: Measurements and thermodynamic modeling. *International Journal of Hydrogen Energy*, *50*, 648-658. doi: 10.1016/j.ijhydene.2023.10.290

Chabab, S., Théveneau, P., Coquelet, C., Corvisier, J., & Paricaud, P. (2020). Measurements and predictive models of high-pressure h2 solubility in brine (h2o+nacl) for underground hydrogen storage application. *International Journal of Hydrogen Energy*, *45*, 32206-32220. doi: 10.1016/j.ijhydene.2020.08.192

Conrad, R. (1999). Contribution of hydrogen to methane production and control of hydrogen concentrations in methanogenic soils and sediments. *FEMS Microbiology Ecology*, *28*, 193-202. doi: 10.1111/j.1574-6941.1999.tb00575.x

Cooke, R. J., Pettini, M., Jorgenson, R. A., Murphy, M. T., & Steidel, C. C. (2014). Precision measures of the primordial abundance of deuterium. *Astrophysical Journal*, *781*. doi: 10.1088/0004-637X/781/1/31

Cox, S. F., & Etheridge, M. A. (1989). Coupled grain-scale dilatancy and mass transfer during deformation at high fluid pressures: examples from mount lyell, tasmania. *Journal of Structural Geology*, *11*, 147-162.

Craig, H., & Lupton, J. (1976). Primordial neon, helium, and hydrogen in oceanic basalts. *Earth and Planetary Science Letters*, *31*, 369-385. doi: https://doi.org/10.1016/0012-821X(76)90118-7

Debaille, V., O'Neill, C., Brandon, A. D., Haenecour, P., Yin, Q. Z., Mattielli, N., & Treiman, A. H. (2013). Stagnant-lid tectonics in early earth revealed by 142nd variations in late archean rocks. *Earth and Planetary Science Letters*, *373*, 83-92. doi: 10.1016/j.epsl.2013.04.016

de Blok, W. J., Fortuin, J. M. H., & Vermeulen, D. P. (1982). Bestimmung des diffusionskoeffizienten von wasserstoff in wasser und w isserigen polymerliisungen nach der cbs-methode measurement of the diffusion coefficient of hydrogen in water ca and aqueous polymer solutions according to the cbs-method. *Wirme und Stofffibertragung*, *17*, 11-16.

Demouchy, S. (2010). Diffusion of hydrogen in olivine grain boundaries and implications for the survival of water-rich zones in the earth's mantle. *Earth and Planetary Science Letters*, *295*, 305-313. doi: 10.1016/j.epsl.2010.04.019

Demouchy, S., & Mackwell, S. (2006). Mechanisms of hydrogen incorporation and diffusion in iron-bearing olivine. *Physics and Chemistry of Minerals*, *33*, 347-355. doi: 10.1007/s00269-006-0081-2

Deronzier, J. F., & Giouse, H. (2020). Vaux-en-bugey (ain, france): The first gas field produced in france, providing learning lessons for natural hydrogen in the sub-surface? *BSGF - Earth Sciences Bulletin*, *191*. doi: 10.1051/bsgf/2020005

Deville, E., & Prinzhofer, A. (2016). The origin of n2-h2-ch4-rich natural gas seepages in ophiolitic context: A major and noble gases study of fluid seepages in new caledonia. *Chemical Geology*, *440*, 139-147. doi: 10.1016/j.chemgeo.2016.06.011

Dodd, M. S., Wang, H., Li, C., Towner, M., Thomson, A. R., Slack, J. F., ... Papineau, D. (2022). Abiotic anoxic iron oxidation, formation of archean banded iron formations, and the oxidation of early earth. *Earth and Planetary Science Letters*, *584*. doi: 10.1016/j.epsl.2022.117469

Donzé, F. V., Truche, L., Namin, P. S., Lefeuvre, N., & Bazarkina, E. F. (2020). Migration of natural hydrogen from deep-seated sources in the são francisco basin, brazil. *Geosciences (Switzerland)*, *10*, 1-16. doi: 10.3390/geosciences10090346

Dopffel, N., Jansen, S., & Gerritse, J. (2021). *Microbial side effects of underground hydrogen storage – knowledge gaps, risks and opportunities for successful implementation* (Vol. 46). Elsevier Ltd. doi: 10.1016/j.ijhydene.2020.12.058

Dutta, A., Gupta, S. D., Gupta, A., Sarkar, J., Roy, S., Mukherjee, A., & Sar, P. (2018). Exploration of deep terrestrial subsurface microbiome in late cretaceous deccan traps and underlying archean basement, india. *Scientific Reports*, *8*. doi: 10.1038/s41598-018-35940-0

Eichhubl, P., & Boles, J. R. (2000). Focused fluid flow along faults in the monterey formation, coastal california. *GSA Bulletin*, 1667-1679. Retrieved from `http://pubs.geoscienceworld.org/gsa/gsabulletin/article-pdf/112/11/1667/3383642/i0016-7606-112-11-1667.pdf`

Escudero, C., Oggerin, M., & Amils, R. (2018). The deep continental subsurface: the dark biosphere. *International Microbiology*, *21*, 3-14. doi: 10.1007/s10123-018-0009-y

Farough, A., Moore, D. E., Lockner, D. A., & Lowell, R. P. (2016). Evolution of fracture permeability of ultramafic rocks undergoing serpentinization at hydrothermal conditions: An experimental study. *Geochemistry, Geophysics, Geosystems*, *17*, 44-55. doi: 10.1002/2015GC005973

Farquhar, J., Wing, B., McKeegan, K., Harris, J., Cartigny, P., & Thiemens, M. (2002). Mass-independent sulfur of inclusions in diamond and sulfur recycling on early earth. *Science*, *298*, 2369-2372.

Farver, J. R. (2010). Oxygen and hydrogen diffusion in minerals. *Reviews in Mineralogy and Geochemistry*, *72*, 447-507. doi: 10.2138/rmg.2010.72.10

Faulkner, D. R., Jackson, C. A., Lunn, R. J., Schlische, R. W., Shipton, Z. K., Wibberley, C. A., & Withjack, M. O. (2010). A review of recent developments concerning the structure, mechanics and fluid flow properties of fault zones. *Journal of Structural Geology*, *32*, 1557-1575. doi: 10.1016/j.jsg.2010.06.009

Ferrell, R. T., & Himmelblau, D. M. (1967). Diffusion coefficients of hydrogen and helium in water. *AIChE Journal*, *13*, 702-708. doi: 10.1002/aic.690130421

Firstov, P., & Shirokov, V. (2005). Dynamics of molecular hydrogen and its relation to deformational processes at the petropavlovsk-kamchatskii geodynamic test site: Evidence from observations in 1999–2003. *Geochemistry International*, *43*, 1056-1064.

French, S. W., & Romanowicz, B. (2015). Broad plumes rooted at the base of the earth's mantle beneath major hotspots. *Nature*, *525*, 95-99. doi: 10.1038/nature14876

Frery, E., Fryer, P., Kurz, W., Nguyen, A., Sissmann, O., Uysal, T., & Zhao, J. (2021). Episodicity of structural flow in an active subduction system, new insights from mud volcano's carbonate veins – scientific ocean drilling expedition iodp 366. *Marine Geology*, *434*. doi: 10.1016/j.margeo.2021.106431

Frery, E., Gratier, J. P., Ellouz-Zimmerman, N., Loiselet, C., Braun, J., Deschamps, P., ... Swennen, R. (2015). Evolution of fault permeability during episodic fluid circulation: Evidence for the effects of fluid-rock interactions from travertine studies (utah-usa). *Tectonophysics*, *651*, 121-137. doi: 10.1016/j.tecto.2015.03.018

Frery, E., Langhi, L., Maison, M., & Moretti, I. (2021). Natural hydrogen seeps identified in the north perth basin, western australia. *International Journal of Hydrogen Energy*, *46*, 31158-31173. doi: 10.1016/j.ijhydene.2021.07.023

Frisch, H. L. (1957). The time lag in diffusion. *The Journal of Physical Chemistry*, *61*, 93-95. Retrieved from `https://pubs.acs.org/sharingguidelines` doi: 10.1021/j150547a018

Garnero, E. J., McNamara, A. K., & Shim, S. H. (2016). *Continent-sized anomalous zones with low seismic velocity at the base of earth's mantle* (Vol. 9). Nature Publishing Group. doi: 10.1038/ngeo2733

Gautheron, C., & Moreira, M. (2002). Helium signature of the subcontinental lithospheric mantle. *Earth and Planetary Science Letters*, *199*, 39-47. Retrieved from `www.elsevier.com/locate/epsl`

Geiss, J., & Gloeckler, G. (1998). Abundances of deuterium and helium-3 in the protosolar cloud. In N. Prantzos, M. Tosi, & R. V. Steiger (Eds.), (1st ed., Vol. 4, p. 239-250). Springer.

Gerya, T. V., Stern, R. J., Baes, M., Sobolev, S. V., & Whattam, S. A. (2015). Plate tectonics on the earth triggered by plume-induced subduction initiation. *Nature*, *527*, 221-225. doi: 10.1038/nature15752

Geymond, U., Ramanaidou, E., Lévy, D., Ouaya, A., & Moretti, I. (2022). Can weathering of banded iron formations generate natural hydrogen? evidence from australia, brazil and south africa. *Minerals*, *12*. doi: 10.3390/min12020163

Gilfillan, S. M., Ballentine, C. J., Holland, G., Blagburn, D., Lollar, B. S., Stevens, S., ... Cassidy, M. (2008). The noble gas geochemistry of natural co2 gas reservoirs from the colorado plateau and rocky mountain provinces, usa. *Geochimica et Cosmochimica Acta*, *72*, 1174-1198. doi: 10.1016/j.gca.2007.10.009

Goh, J. (2023). *Gold hydrogen detects significant concentrations of hydrogen and helium at ramsay 1 well.* Retrieved from `https://www.proactiveinvestors.com.au/companies/news/1031450/gold-hydrogen-detects-significant-concentrations-of-hydrogen-and-helium-at-ramsay-1-well-1031450`

.html

Gonnermann, H. M., & Mukhopadhyay, S. (2007). Non-equilibrium degassing and a primordial source for helium in ocean-island volcanism. *Nature*, *449*, 1037-1040. doi: 10.1038/nature06240

Graham, D. W. (2002). Noble gas isotope geochemistry of mid-ocean ridge and ocean island basalts: Characterization of mantle source reservoirs. *Reviews in Mineralogy and Geochemistry*, *47*. doi: 10.2138/rmg.2002.47.8

Gratier, J.-P., & Gueydan, F. (2007). Deformation in the presence of fluids and mineral reactions effect of fracturing and fluid-rock interaction on seismic cycles. In (Vol. 95, p. 319-356).

Greenberger, R. N., Mustard, J. F., Cloutis, E. A., Pratt, L. M., Sauer, P. E., Mann, P., ... Bish, D. L. (2015). Serpentinization, iron oxidation, and aqueous conditions in an ophiolite: Implications for hydrogen production and habitability on mars. *Earth and Planetary Science Letters*, *416*, 21-34. doi: 10.1016/j.epsl.2015.02.002

Greening, C., Biswas, A., Carere, C. R., Jackson, C. J., Taylor, M. C., Stott, M. B., ... Morales, S. E. (2016). Genomic and metagenomic surveys of hydrogenase distribution indicate h2 is a widely utilised energy source for microbial growth and survival. *ISME Journal*, *10*, 761-777. doi: 10.1038/ismej.2015.153

Gregory, S. P., Barnett, M. J., Field, L. P., & Milodowski, A. E. (2019). Subsurface microbial hydrogen cycling: Natural occurrence and implications for industry. *Microorganisms*, *7*. doi: 10.3390/microorganisms7020053

Hancock, P. L., Chalmers, R. M. L., Altunel, E., & Cakir, Z. (1999). Travitonics: using travertines in active fault studies. *Journal of Structural Geology*, *21*, 903-916. Retrieved from www.elsevier.nl/locate/jstrugeo

Hand, E. (2023). Hidden hydrogen: Does earth hold vast stores of a renewable, carbon-free fuel? *Science*, *379*, 631-636.

Hantschel, T., & Kauerauf, A. (2009). *Fundamentals of basin and petroleum systems modeling*. Springer.

Harris, S. H., Smith, R. L., & Suflita, J. M. (2007). In situ hydrogen consumption kinetics as an indicator of subsurface microbial activity. *FEMS Microbiology Ecology*, *60*, 220-228. doi: 10.1111/j.1574-6941.2007.00286.x

Hemme, C., & van Berk, W. (2018). Hydrogeochemical modeling to identify potential risks of underground hydrogen storage in depleted gas fields. *Applied Sciences (Switzerland)*, *8*. doi: 10.3390/app8112282

Hilton, D. R., Hammerschmidt, K., Loock, G., & Priedrichsen, H. (1993). Helium and argon isotope systematics of the central lau basin and valu fa ridge: Evidence of crust/mantle interactions in a back-arc basin. *Geochimica et Cosmochimica Acta*, *57*, 2819-2841.

Holm, N. G., Oze, C., Mousis, O., Waite, J. H., & Guilbert-Lepoutre, A. (2015). Serpentinization and the formation of h2 and ch4 on celestial bodies (planets, moons, comets). *Astrobiology*, *15*, 587-600. doi: 10.1089/ast.2014.1188

Hopp, J., & Trieloff, M. (2008). Helium deficit in high-3he/4he parent magmas: Predegassing fractionation, not a "helium paradox". *Geochemistry, Geophysics, Geosystems*, *9*. doi: 10.1029/2007GC001833

Horsfield, B., Mahlstedt, N., Weniger, P., Misch, D., Vranjes-Wessely, S., Han, S., & Wang, C. (2022). Molecular hydrogen from organic sources in the deep songliao basin, p.r. china. *International Journal of Hydrogen Energy*, *47*, 16750-16774. doi: 10.1016/j.ijhydene.2022.02.208

Hosgörmez, H. (2007). Origin of the natural gas seep of Çirali (chimera), turkey: Site of the first olympic fire. *Journal of Asian Earth Sciences*, *30*, 131-141. doi: 10.1016/j.jseaes.2006.08.002

Hoskin, C. M., & Sundeen, D. A. (1985). Grain size of granite and derived grus, enchanted rock pluton, texas. *Sedimentary Geology*, *42*, 25-40.

Hosseini, M., Fahimpour, J., Ali, M., Keshavarz, A., & Iglauer, S. (2022). H2-brine

interfacial tension as a function of salinity, temperature, and pressure; implications for hydrogen geo-storage. *Journal of Petroleum Science and Engineering*, *213*. doi: 10.1016/j.petrol.2022.110441

Huang, S., Lee, C. T. A., & Yin, Q. Z. (2014). Missing lead and high 3he/4he in ancient sulfides associated with continental crust formation. *Scientific Reports*, *4*. doi: 10.1038/srep05314

Hutchinson, I. P., Jackson, O., Stocks, A. E., Barnicoat, A. C., & Lawrence, S. R. (2024). Greenstones as a source of hydrogen in cratonic sedimentary basins. *Geological Society, London, Special Publications*, *547*. Retrieved from `https://www.lyellcollection.org/doi/10.1144/SP547-2023-39` doi: 10.1144/SP547-2023-39

Hydrogen, G. (2023). *Exploration update: Very high helium concentrations found at ramsay 2.* Retrieved from `https://www.goldhydrogen.com.au/wp/wp-content/uploads/2023.12.06-ASX-Announcement-Very-High-Helium-Concentrations-at-Ramsay-2.pdf`

IEA. (2021). *Global hydrogen review 2021.* Retrieved from `https://iea.blob.core.windows.net/assets/5bd46d7b-906a-4429-abda-e9c507a62341/GlobalHydrogenReview2021.pdf`

Iglauer, S., Mathew, M. S., & Bresme, F. (2012). Molecular dynamics computations of brine-co2 interfacial tensions and brine-co2-quartz contact angles and their effects on structural and residual trapping mechanisms in carbon geo-sequestration. *Journal of Colloid and Interface Science*, *386*, 405-414. doi: 10.1016/j.jcis.2012.06.052

Ireland, M. T., Morley, C. K., & Davies, R. J. (2021). Systematic spacing and topological variations in layer-bound fault systems. *Basin Research*, *33*, 2745-2762. doi: 10.1111/bre.12582

Jackson, M. G., Konter, J. G., & Becker, T. W. (2017). Primordial helium entrained by the hottest mantle plumes. *Nature*, *542*, 340-343. doi: 10.1038/nature21023

Jacops, E., Aertsens, M., Maes, N., Bruggeman, C., Krooss, B. M., Amann-Hildenbrand, A., ... Littke, R. (2017). Interplay of molecular size and pore network geometry on the diffusion of dissolved gases and hto in boom clay. *Applied Geochemistry*, *76*, 182-195. doi: 10.1016/j.apgeochem.2016.11.022

Jimenez-Rodriguez, S., Quade, J., Levin, N. E., Campisano, C. J., Stinchcomb, G. E., Roman, D. C., & Bedaso, Z. (2023). Environmental controls on the hydrogen isotopic composition of volcanic glass from the southern afar rift, eastern ethiopia. *Chemical Geology*, *628*. doi: 10.1016/j.chemgeo.2023.121484

Johnson, T. E., Brown, M., Gardiner, N. J., Kirkland, C. L., & Smithies, R. H. (2017). Earth's first stable continents did not form by subduction. *Nature*, *543*, 239-242. doi: 10.1038/nature21383

Kalati, S. S., Khiabani, N. P., Ayatollahi, S., Mahani, H., Zivar, D., & Esmaeilbeig, M. A. (2024). Molecular dynamics simulation of hydrogen diffusion into brine: Implications for underground hydrogen storage. *International Journal of Hydrogen Energy*, *53*, 17-28. doi: 10.1016/j.ijhydene.2023.11.318

Kampman, N., Burnside, N. M., Shipton, Z. K., Chapman, H. J., Nicholl, J. A., Ellam, R. M., & Bickle, M. J. (2012). Pulses of carbon dioxide emissions from intracrustal faults following climatic warming. *Nature Geoscience*, *5*, 352-358. doi: 10.1038/ngeo1451

Karato, S. (2007). Microscopic models for the effects of hydrogen on physical and chemical properties of earth materials. In D. Yuen, S. Maruyama, S. Karato, & B. Windley (Eds.), (p. 321-351). Springer.

Karolytė, R., Warr, O., van Heerden, E., Flude, S., de Lange, F., Webb, S., ... Lollar, B. S. (2022). The role of porosity in h2/he production ratios in fracture fluids from the witwatersrand basin, south africa. *Chemical Geology*, *595*. doi: 10.1016/j.chemgeo.2022.120788

Kellogg, L. H., & Wasserburg, G. J. (1990). *The role of plumes in mantle helium fluxes.* Elsevier Science Publishers B.V.

Keshavarz, A., Abid, H., Ali, M., & Iglauer, S. (2022). Hydrogen diffusion in coal: Implications for hydrogen geo-storage. *Journal of Colloid and Interface Science*, *608*, 1457-1462. doi: 10.1016/j.jcis.2021.10.050

Klein, F., Bach, W., & McCollom, T. M. (2013). Compositional controls on hydrogen generation during serpentinization of ultramafic rocks. *Lithos*, *178*, 55-69. doi: 10.1016/j.lithos.2013.03.008

Kohlstedt, D., & Mackwell, S. (1998). Diffusion of hydrogen and intrinsic point defects in olivine. *Zeitschrift für physikalische Chemie*, *207*, 147-162.

Koproch, N., Dahmke, A., & Köber, R. (2019). The aqueous solubility of common organic groundwater contaminants as a function of temperature between 5 and 70 c. *Chemosphere*, *217*, 166-175. doi: 10.1016/j.chemosphere.2018.10.153

Kotelnikova, S., & Pedersen, K. (1998). Distribution and activity of methanogens and homoacetogens in deep granitic aquifers at aspo hard rock laboratory, sweden. *FEMS Microbiology Ecology*, *26*, 121-134. doi: 10.1111/j.1574-6941.1998.tb00498.x

Kufner, S. K., Kakar, N., Bezada, M., Bloch, W., Metzger, S., Yuan, X., ... Schurr, B. (2021). The hindu kush slab break-off as revealed by deep structure and crustal deformation. *Nature Communications*, *12*. doi: 10.1038/s41467-021-21760-w

Kurz, M. D., Jenkins, W. J., & Hart, S. R. (1982). *Helium isotopic systematics of oceanic islands and mantle heterogeneity* (Vol. 297).

Lamadrid, H. M., Rimstidt, J. D., Schwarzenbach, E. M., Klein, F., Ulrich, S., Dolocan, A., & Bodnar, R. J. (2017). Effect of water activity on rates of serpentinization of olivine. *Nature Communications*, *8*. doi: 10.1038/ncomms16107

Lefeuvre, N., Truche, L., Donzé, F. V., Ducoux, M., Barré, G., Fakoury, R. A., ... Gaucher, E. C. (2021). Native h2 exploration in the western pyrenean foothills. *Geochemistry, Geophysics, Geosystems*, *22*, 1-20. doi: 10.1029/2021GC009917

Lefeuvre, N., Truche, L., Donzé, F. V., Gal, F., Tremosa, J., Fakoury, R. A., ... Gaucher, E. C. (2022). Natural hydrogen migration along thrust faults in foothill basins: The north pyrenean frontal thrust case study. *Applied Geochemistry*, *145*. doi: 10.1016/j.apgeochem.2022.105396

Li, J., & Chou, I. M. (2015). Hydrogen in silicate melt inclusions in quartz from granite detected with raman spectroscopy. *Journal of Raman Spectroscopy*, *46*, 983-986. doi: 10.1002/jrs.4644

Lin, L. H., Slater, G. F., Lollar, B. S., Lacrampe-Couloume, G., & Onstott, T. C. (2005). The yield and isotopic composition of radiolytic h2, a potential energy source for the deep subsurface biosphere. *Geochimica et Cosmochimica Acta*, *69*, 893-903. doi: 10.1016/j.gca.2004.07.032

Lin, S. C., & Keken, P. E. V. (2006). Dynamics of thermochemical plumes: 1. plume formation and entrainment of a dense layer. *Geochemistry, Geophysics, Geosystems*, *7*. doi: 10.1029/2005GC001071

Lis, D. C., Bockelée-Morvan, D., Güsten, R., Biver, N., Stutzki, J., Delorme, Y., ... Okada, Y. (2019). Terrestrial deuterium-to-hydrogen ratio in water in hyperactive comets. *Astronomy and Astrophysics*, *625*. doi: 10.1051/0004-6361/201935554

Liu, J., Wang, S., Javadpour, F., Feng, Q., & Cha, L. (2022). Hydrogen diffusion in clay slit: Implications for the geological storage. *Energy and Fuels*, *36*, 7651-7660. doi: 10.1021/acs.energyfuels.2c01189

Liu, Z., Perez-Gussinye, M., García-Pintado, J., Mezri, L., & Bach, W. (2023). Mantle serpentinization and associated hydrogen flux at north atlantic magma-poor rifted margins. *Geology*, *51*, 284-289. doi: 10.1130/G50722.1

Lodhia, B. H. (2023). *hydrogen_mobility (version 1.0.0) [computer software].* Re-

trieved from https://zenodo.org/doi/10.5281/zenodo.10990920https://github.com/lodhia92/hydrogen_mobility doi: 10.5281/zenodo.10990920

Lodhia, B. H., & Clark, S. R. (2022). Computation of vertical fluid mobility of co2 , methane , hydrogen and hydrocarbons through sandstones and carbonates. *Scientific Reports*, 1-14. Retrieved from https://doi.org/10.1038/s41598-022-14234-6 doi: 10.1038/s41598-022-14234-6

Lodhia, B. H., & Peeters, L. (2024). The migration of hydrogen in sedimentary basins. *Australian Energy Producers Journal*.

Loewen, M. W., Graham, D. W., Bindeman, I. N., Lupton, J. E., & Garcia, M. O. (2019). Hydrogen isotopes in high 3 he/ 4 he submarine basalts: Primordial vs. recycled water and the veil of mantle enrichment. *Earth and Planetary Science Letters*, *508*, 62-73. doi: 10.1016/j.epsl.2018.12.012

Lollar, B. S., Onstott, T. C., Lacrampe-Couloume, G., & Ballentine, C. J. (2014). The contribution of the precambrian continental lithosphere to global h2 production. *Nature*, *516*, 379-382. doi: 10.1038/nature14017

Lopez-Lazaro, C., Bachaud, P., Moretti, I., & Ferrando, N. (2019). Predicting the phase behavior of hydrogen in nacl brines by molecular simulation for geological applications. *BSGF - Earth Sciences Bulletin*, *190*. doi: 10.1051/bsgf/2019008

Lupton, J., & Craig, H. (1975). Excess 3he in oceanic basalts: Evidence for terrestrial primordial helium. *Earth and Planetary Science Letters*, *26*, 133-139. doi: https://doi.org/10.1016/0012-821x(75)90080-1

Lévy, D., Boka-Mene, M., Meshi, A., Fejza, I., Guermont, T., Hauville, B., & Pelissier, N. (2023). Looking for natural hydrogen in albania and kosova. *Frontiers in Earth Science*, *11*. doi: 10.3389/feart.2023.1167634

Mackintosh, S. J., & Ballentine, C. J. (2012). Using 3he/ 4he isotope ratios to identify the source of deep reservoir contributions to shallow fluids and soil gas. *Chemical Geology*, *304-305*, 142-150. doi: 10.1016/j.chemgeo.2012.02.006

Magnabosco, C., Lin, L. H., Dong, H., Bomberg, M., Ghiorse, W., Stan-Lotter, H., ... Onstott, T. C. (2018). *The biomass and biodiversity of the continental subsurface* (Vol. 11). Nature Publishing Group. doi: 10.1038/s41561-018-0221-6

Mahlstedt, N., Horsfield, B., Weniger, P., Misch, D., Shi, X., Noah, M., & Boreham, C. (2022). Molecular hydrogen from organic sources in geological systems. *Journal of Natural Gas Science and Engineering*, *105*. doi: 10.1016/j.jngse.2022.104704

Mangenot, X., Xie, H., Crémière, A., Giunta, T., Lilley, M., Sissmann, O., ... Eiler, J. (2023). 2h-2h clumping in molecular hydrogen method and preliminary results. *Chemical Geology*, *621*. doi: 10.1016/j.chemgeo.2022.121278

Marcaillou, C., Muñoz, M., Vidal, O., Parra, T., & Harfouche, M. (2011). Mineralogical evidence for h2 degassing during serpentinization at 300°c/300bar. *Earth and Planetary Science Letters*, *303*, 281-290. doi: 10.1016/j.epsl.2011.01.006

Marques, J. M., Etiope, G., Neves, M. O., Carreira, P. M., Rocha, C., Vance, S. D., ... Suzuki, S. (2018). Linking serpentinization, hyperalkaline mineral waters and abiotic methane production in continental peridotites: an integrated hydrogeological-bio-geochemical model from the cabeço de vide ch4-rich aquifer (portugal). *Applied Geochemistry*, *96*, 287-301. doi: 10.1016/j.apgeochem.2018.07.011

Marty, B. (2012). The origins and concentrations of water, carbon, nitrogen and noble gases on earth. *Earth and Planetary Science Letters*, *313-314*, 56-66. doi: 10.1016/j.epsl.2011.10.040

Marty, B., & Yokochi, R. (2006). Water in the early earth. *Reviews in Mineralogy & Geochemistry*, *62*, 421-450. doi: 10.2138/rmg.2006.62.18

Massiot, C., Seebeck, H., Nicol, A., McNamara, D. D., Lawrence, M. J., Griffin, A. G., ... Viskovic, G. P. D. (2019). Effects of regional and local stresses on

fault slip tendency in the southern taranaki basin, new zealand. *Marine and Petroleum Geology*, *107*, 467-483. doi: 10.1016/j.marpetgeo.2019.05.030

Mathiesen, J., Linga, G., Misztal, M., Renard, F., & Borgne, T. L. (2023). Dynamic fluid connectivity controls solute dispersion in multiphase porous media flow. *Geophysical Research Letters*, *50*. doi: 10.1029/2023GL105233

McCollom, T. M., & Amend, J. P. (2005). A thermodynamic assessment of energy requirements for biomass synthesis by chemolithoautotrophic microorganisms in oxic and anoxic environments. *Geobiology*, *3*, 135-144. doi: 10.1111/j.1472-4669.2005.00045.x

Moretti, I., Brouilly, E., Loiseau, K., Prinzhofer, A., & Deville, E. (2021). Hydrogen emanations in intracratonic areas: New guide lines for early exploration basin screening. *Geosciences*, *11*. doi: 10.3390/geosciences11030145

Moretti, I., Prinzhofer, A., Françolin, J., Pacheco, C., Rosanne, M., Rupin, F., & Mertens, J. (2021). Long-term monitoring of natural hydrogen superficial emissions in a brazilian cratonic environment. sporadic large pulses versus daily periodic emissions. *International Journal of Hydrogen Energy*, *46*, 3615-3628. doi: 10.1016/j.ijhydene.2020.11.026

Morgan, W. (1971). Convection plumes in the lower mantle. *Nature*, *230*, 42-43.

Mostinsky, I. L. (2011). Diffusion coefficient. Begellhouse. doi: 10.1615/AtoZ.d.diffusion_coefficient

Muhammed, N. S., Haq, B., Shehri, D. A., Al-Ahmed, A., Rahman, M. M., & Zaman, E. (2022). A review on underground hydrogen storage: Insight into geological sites, influencing factors and future outlook. *Energy Reports*, *8*, 461-499. doi: 10.1016/j.egyr.2021.12.002

Mukhopadhyay, S. (2012). Early differentiation and volatile accretion recorded in deep-mantle neon and xenon. *Nature*, *486*, 101-104. doi: 10.1038/nature11141

Myagkiy, A., Brunet, F., Popov, C., Krüger, R., Guimarães, H., Sousa, R. S., ... Moretti, I. (2020). H2 dynamics in the soil of a h2-emitting zone (são francisco basin, brazil): Microbial uptake quantification and reactive transport modelling. *Applied Geochemistry*, *112*. doi: 10.1016/j.apgeochem.2019.104474

Myagkiy, A., Moretti, I., & Brunet, F. (2020). Space and time distribution of subsurface h2concentration in so-called "fairy circles": Insight from a conceptual 2-d transport model. *BSGF - Earth Sciences Bulletin*, *191*. doi: 10.1051/bsgf/2020010

Nealson, K. H., Inagaki, F., & Takai, K. (2005). Hydrogen-driven subsurface lithoautotrophic microbial ecosystems (slimes): Do they exist and why should we care? *Trends in Microbiology*, *13*, 405-410. doi: 10.1016/j.tim.2005.07.010

Neelameggham, N. R., Subramanian, G., & Kalamegham, P. (2022). Thermoeconomic dynamics of energy-efficient orange hydrogen production: An energy matter. *JOM*, *74*, 1923-1931. doi: 10.1007/s11837-022-05162-x

Nestola, F., & Smyth, J. R. (2016). *Diamonds and water in the deep earth: A new scenario* (Vol. 58). Taylor and Francis Inc. doi: 10.1080/00206814.2015.1056758

Niwa, M., Kurosawa, H., Shimada, K., Ishimaru, T., & Kosaka, H. (2011). Identification of pathways for hydrogen gas migration in fault zones with a discontinuous, heterogeneous permeability structure and the relationship to particle size distribution of fault materials. *Pure and Applied Geophysics*, *168*, 887-900. doi: 10.1007/s00024-010-0167-0

Nova, A., Prifti, K., Negri, F., & Manenti, F. (2023). Multiscale techno-economic analysis of orange hydrogen synthesis. *Energy*, *282*. doi: 10.1016/j.energy.2023.128644

of Energy, U. D. (2024). *U.s. department of energy announces $20 million to 16 projects spearheading exploration of geologic hydrogen.* Retrieved from `https://arpa-e.energy.gov/news-and-media/press-releases/us`

-department-energy-announces-20-million-16-projects-spearheading

O'hanley, D. S. (1992). Solution to the volume problem in serpentinization. *Geology*, *20*, 705-708. Retrieved from http://pubs.geoscienceworld.org/gsa/geology/article-pdf/20/8/705/3513947/i0091-7613-20-8-705.pdf

Olson, P. L., & Sharp, Z. D. (2022). Primordial helium-3 exchange between earth's core and mantle. *Geochemistry, Geophysics, Geosystems*, *23*. doi: 10.1029/2021GC009985

Osselin, F., Pichavant, M., Champallier, R., Ulrich, M., & Raimbourg, H. (2022). Reactive transport experiments of coupled carbonation and serpentinization in a natural serpentinite. implication for hydrogen production and carbon geological storage. *Geochimica et Cosmochimica Acta*, *318*, 165-189. doi: 10.1016/j.gca.2021.11.039

Owczarek, E., & Zakroczymski, T. (2000). Hydrogen transport in a duplex stainless steel. *Acta mater*, *48*, 3059-3070. Retrieved from www.elsevier.com/locate/actamat

Parnell, J., & Blamey, N. (2017). Global hydrogen reservoirs in basement and basins. *Geochemical Transactions*, *18*. doi: 10.1186/s12932-017-0041-4

Perchuk, A. L., Zakharov, V. S., Gerya, T. V., & Griffin, W. L. (2023). Flat subduction in the early earth: The key role of discrete eclogitization kinetics. *Gondwana Research*, *119*, 186-203. doi: 10.1016/j.gr.2023.03.015

Peslier, A. H., & Bizimis, M. (2015). Water in hawaiian peridotite minerals: A case for a dry metasomatized oceanic mantle lithosphere. *Geochemistry, Geophysics, Geosystems*, *16*, 1211-1232. doi: 10.1002/2015GC005780

Peslier, A. H., Schönbächler, M., Busemann, H., & Karato, S. I. (2017). Water in the earth's interior: Distribution and origin. *Space Science Reviews*, *212*, 743-810. doi: 10.1007/s11214-017-0387-z

Pinti, D. L. (2021). Deuterium/hydrogen ratio. in: , et al. In (p. 1-3). Retrieved from https://link.springer.com/referenceworkentry/10.1007/978-3-642-278... doi: 10.1007/978-3-642-278

Polat, A., & Hofmann, A. W. (2003). Alteration and geochemical patterns in the 3.7-3.8 ga isua greenstone belt, west greenland. In (Vol. 126, p. 197-218). Elsevier B.V. doi: 10.1016/S0301-9268(03)00095-0

Porcelli, D., & Elliott, T. (2008, 5). The evolution of he isotopes in the convecting mantle and the preservation of high 3he/4he ratios. *Earth and Planetary Science Letters*, *269*, 175-185. doi: 10.1016/j.epsl.2008.02.002

Poreda, R., Schilling, J.-G., & Craig, H. (1986). Helium and hydrogen isotopes in ocean-ridge basalts north and south of iceland. *Earth and Planetary Science Letters*, *78*, 1-17. doi: https://doi.org/10.1016/0012-821X(86)90168-8

Prinzhofer, A., & Cacas-Stentz, M. C. (2023). Natural hydrogen and blend gas: a dynamic model of accumulation. *International Journal of Hydrogen Energy*, *48*, 21610-21623. doi: 10.1016/j.ijhydene.2023.03.060

Prinzhofer, A., Cissé, C. S. T., & Diallo, A. B. (2018). Discovery of a large accumulation of natural hydrogen in bourakebougou (mali). *International Journal of Hydrogen Energy*, *43*, 19315-19326. doi: 10.1016/j.ijhydene.2018.08.193

Prinzhofer, A., Moretti, I., Françolin, J., Pacheco, C., D'Agostino, A., Werly, J., & Rupin, F. (2019). Natural hydrogen continuous emission from sedimentary basins: The example of a brazilian h 2 -emitting structure. *International Journal of Hydrogen Energy*, *44*, 5676-5685. doi: 10.1016/j.ijhydene.2019.01.119

Renard, F., Candela, T., & Bouchaud, E. (2013). Constant dimensionality of fault roughness from the scale of micro-fractures to the scale of continents. *Geophysical Research Letters*, *40*, 83-87. doi: 10.1029/2012GL054143

Rezaee, R. (2021). Assessment of natural hydrogen systems in western australia. *International Journal of Hydrogen Energy*, *46*, 33068-33077. doi: 10.1016/j.ijhydene.2021.07.149

Rhode, M., Richter, T., Mente, T., Mayr, P., & Nitsche, A. (2022). Thickness

and microstructure effect on hydrogen diffusion in creep-resistant 9 % cr p92 steel and p91 weld metal. *Welding in the World*, *66*, 325-340. doi: 10.1007/s40194-021-01218-9

Rison, W., & Craig, H. (1983). *Helium isotopes and mantle volatiles in loihi seamount and hawaiian island basalts and xenoliths* (Vol. 66).

Roden, E. E., & Jin, Q. (2011, 3). Thermodynamics of microbial growth coupled to metabolism of glucose, ethanol, short-chain organic acids, and hydrogen. *Applied and Environmental Microbiology*, *77*, 1907-1909. doi: 10.1128/AEM.02425-10

Rouméjon, S., & Cannat, M. (2014). Serpentinization of mantle-derived peridotites at mid-ocean ridges: Mesh texture development in the context of tectonic exhumation. *Geochemistry, Geophysics, Geosystems*, *15*, 2354-2379. doi: 10.1002/2013GC005148

Roy, S., Raju, R., Chuang, H. F., Cruden, B. A., & Meyyappan, M. (2003). Modeling gas flow through microchannels and nanopores. *Journal of Applied Physics*, *93*, 4870-4879. doi: 10.1063/1.1559936

Sakhaee-Pour, A., & Alessa, S. (2022). Hydrogen permeability in subsurface. *International Journal of Hydrogen Energy*, *47*, 27071-27079. doi: 10.1016/j.ijhydene .2022.06.042

Salerno, E., Bühler, F., Bochsler, P., Busemann, H., Bassi, M., Zastenker, G., ... Eismont, N. (2003). Measurement of 3he/4he in the local interstellar medium: The collisa experiment on mir. *The Astrophysical Journal*, *585*, 840.

Samuel, H., & Farnetani, C. G. (2003). Thermochemical convection and helium concentrations in mantle plumes. *Earth and Planetary Science Letters*, *207*, 39-56. doi: 10.1016/S0012-821X(02)01125-1

Sano, Y., Urabe, A., & Wakita, H. (1993). Origin of hydrogen-nitrogen gas seeps, oman hisao wushiki . *Applied Geochemistry*, *8*, 1-8.

Schink, B., Thiemann, V., Laue, H., & Friedrich, M. W. (2002). Desulfotignum phosphitoxidans sp. nov., a new marine sulfate reducer that oxidizes phosphite to phosphate. *Archives of Microbiology*, *177*, 381-391. doi: 10.1007/s00203-002-0402-x

Schlinger, C. M., Rosenbaum, J. G., & Veblen, D. R. (1988). Fe-oxide microcrystals in welded tuff from southern nevada: Origin of remanence carriers by precipitation in volcanic glass. *Geology*, *16*, 556-559. Retrieved from `http://pubs.geoscienceworld.org/gsa/geology/article-pdf/16/6/556/3510934/i0091-7613-16-6-556.pdf`

Seton, M., Müller, R. D., Zahirovic, S., Williams, S. E., Nicky, M. W., Cannon, J., ... McGirr, R. (2020). A global data set of present-day oceanic crustal age and seafloor spreading parameters. *Geochemistry, Geophysics, Geosystems*, *21*. doi: 10.1029/2020GC009214

Sharapov, V., Semenov, Y., Kuznetsov, G., & Boguslavsky, A. (2022). Spinel crystals in mantle ultramafic xenoliths as the source of p-t conditions of alteration above the magma chamber beneath the avacha volcano (kamchatka). *Journal of Asian Earth Sciences: X*, *8*. doi: 10.1016/j.jaesx.2022.100119

Shaw, A. M., Hauri, E. H., Fischer, T. P., Hilton, D. R., & Kelley, K. A. (2008). Hydrogen isotopes in mariana arc melt inclusions: Implications for subduction dehydration and the deep-earth water cycle. *Earth and Planetary Science Letters*, *275*, 138-145. doi: 10.1016/j.epsl.2008.08.015

Shirey, S., & S.H., R. (2011). Start of the wilson cycle at 3 ga shown by diamonds from subcontinental mantle. *Science*, *333*, 434-436. doi: 10.1126/science.1204255

Smithies, R. H., Champion, D. C., & Cassidy, K. F. (2003). Formation of earth's early archaean continental crust. *Precambrian Research*, *127*, 89-101. doi: 10 .1016/S0301-9268(03)00182-7

Solomatov, V. S., & Moresi, L. N. (2000). Scaling of time-dependent stagnant lid

convection: Application to small-scale convection on earth and other terrestrial planets. *Journal of Geophysical Research: Solid Earth*, *105*, 21795-21817. doi: 10.1029/2000jb900197

Solum, J. G., Davatzes, N. C., & Lockner, D. A. (2010). Fault-related clay authigenesis along the moab fault: Implications for calculations of fault rock composition and mechanical and hydrologic fault zone properties. *Journal of Structural Geology*, *32*, 1899-1911. doi: 10.1016/j.jsg.2010.07.009

Speciale, P. A., Behr, W. M., Hirth, G., & Tokle, L. (2020). Rates of olivine grain growth during dynamic recrystallization and postdeformation annealing. *Journal of Geophysical Research: Solid Earth*, *125*. doi: 10.1029/2020JB020415

Sperner, B., Lorenz, F., Bonjer, K., Hettel, S., Müller, B., & Wenzel, F. (2001). Slab break-off - abrupt cut or gradual detachment? new insights from the vrancea region (se carpathians, romania). *Terra Nova*, *13*, 172-179. doi: 10.1046/j.1365-3121.2001.00335.x

Stevens, T. O., & McKinley, J. P. (2000). Abiotic controls on h2 production from basalt - water reactions and implications for aquifer biogeochemistry. *Environmental Science and Technology*, *34*, 826-831. doi: 10.1021/es990583g

Strauch, B., Pilz, P., Hierold, J., & Zimmer, M. (2023). Experimental simulations of hydrogen migration through potential storage rocks. *International Journal of Hydrogen Energy*, *48*, 25808-25820. doi: 10.1016/j.ijhydene.2023.03.115

Su, Q., Zeller, E., & Angino, E. (1992). Inducing action of hydrogen migrating along faults on earthquakes. *Acta Seismologica Sinica*, *5*, 841-847. doi: 10.1007/BF02651032

Takai, K., Gamo, T., Tsunogai, U., Nakayama, N., Hirayama, H., Nealson, K. H., & Horikoshi, K. (2004). Geochemical and microbiological evidence for a hydrogen-based, hyperthermophilic subsurface lithoautotrophic microbial ecosystem (hyperslime) beneath an active deep-sea hydrothermal field. *Extremophiles*, *8*, 269-282. doi: 10.1007/s00792-004-0386-3

Templeton, A. S., Ellison, E. T., Kelemen, P. B., Leong, J., Boyd, E. S., Colman, D. R., & Matter, J. M. (2024). Low-temperature hydrogen production and consumption in partially-hydrated peridotites in oman: implications for stimulated geological hydrogen production. *Frontiers in Geochemistry*, *2*. Retrieved from `https://www.frontiersin.org/articles/10.3389/fgeoc.2024.1366268/full` doi: 10.3389/fgeoc.2024.1366268

Thauer, R. K., Jungermann, K., & Decker, K. (1977). Energy conservation in chemotrophic anaerobic bacteria. *Bacteriological Reviews*, *41*, 100-180. Retrieved from `https://journals.asm.org/journal/br`

ToolBox, E. (2018). *Air - diffusion coefficients of gases in excess of air.*

Torres, M. E. S., Saucedo-Vázquez, J. P., & Kroneck, P. M. H. (2015). The magic of dioxygen. In M. S. Torres (Ed.), (Vol. 15, p. 1-12). Springer. doi: 10.1007/978-3-319-12415-5_1

Truche, L., Donzé, F.-V., Goskolli, E., Muceku, B., Loisy, C., Monnin, C., ... Cerepi, A. (2024). A deep reservoir for hydrogen drives intense degassing in the bulqizë ophiolite. *Science*, *383*, 618-621. Retrieved from `https://www.science.org` doi: 10.1126/science.adk9099

Truche, L., Joubert, G., Dargent, M., Martz, P., Cathelineau, M., Rigaudier, T., & Quirt, D. (2018, 7). Clay minerals trap hydrogen in the earth's crust: Evidence from the cigar lake uranium deposit, athabasca. *Earth and Planetary Science Letters*, *493*, 186-197. doi: 10.1016/j.epsl.2018.04.038

Vacquand, C., Deville, E., Beaumont, V., Guyot, F., Sissmann, O., Pillot, D., ... Prinzhofer, A. (2018). Reduced gas seepages in ophiolitic complexes: Evidences for multiple origins of the h2-ch4-n2 gas mixtures. *Geochimica et Cosmochimica Acta*, *223*, 437-461. doi: 10.1016/j.gca.2017.12.018

van der Meer, D. G., van Hinsbergen, D. J., & Spakman, W. (2018). Atlas of the underworld: Slab remnants in the mantle, their sinking history, and a

new outlook on lower mantle viscosity. *Tectonophysics*, *723*, 309-448. doi: 10.1016/j.tecto.2017.10.004

van Hunen, J., & van den Berg, A. P. (2008). Plate tectonics on the early earth: Limitations imposed by strength and buoyancy of subducted lithosphere. *Lithos*, *103*, 217-235. doi: 10.1016/j.lithos.2007.09.016

Vinsot, A., Appelo, C. A., Lundy, M., Wechner, S., Lettry, Y., Lerouge, C., ... Delay, J. (2014). In situ diffusion test of hydrogen gas in the opalinus clay. *Geological Society Special Publication*, *400*, 563-578. doi: 10.1144/SP400.12

Wakita, H., Nakamura, Y., Kita, I., Fujii, N., & Notsu, K. (1980). Hydrogen release: New indicator of fault activity. *Science*, *210*, 188-190. Retrieved from `https://www.science.org`

Wan, B., Yang, X., Tian, X., Yuan, H., Kirscher, U., & Mitchell, R. N. (2020). *Seismological evidence for the earliest global subduction network at 2 ga ago* (Vol. 6). Retrieved from `https://www.science.org`

Wang, C., Zhao, Y., Wu, R., Bi, J., & Zhang, K. (2024). Shale reservoir storage of hydrogen: Adsorption and diffusion on shale. *Fuel*, *357*. doi: 10.1016/j.fuel.2023.129919

Wang, L., Cheng, J., Jin, Z., Sun, Q., Zou, R., Meng, Q., ... Zhang, Q. (2023). High-pressure hydrogen adsorption in clay minerals: Insights on natural hydrogen exploration. *Fuel*, *344*. doi: 10.1016/j.fuel.2023.127919

Wang, L., Jin, Z., Chen, X., Su, Y., & Huang, X. (2023). The origin and occurrence of natural hydrogen. *Energies*, *16*. doi: 10.3390/en16052400

Wang, Z., & Becker, H. (2013). Ratios of s, se and te in the silicate earth require a volatile-rich late veneer. *Nature*, *499*, 328-331. doi: 10.1038/nature12285

Williams, Q., & Hemley, R. J. (2001). Hydrogen in the deep earth. *Annual Review Earth Planetary Sciences*, *29*, 365-418. Retrieved from `www.annualreviews.org`

Xia, Y., Yang, J., Chen, Y., Lu, S., Wang, M., Deng, S., ... Lu, M. (2022). A review of the global polygonal faults: Are they playing a big role in fluid migration? *Frontiers in Earth Science*, *9*. doi: 10.3389/feart.2021.786915

Yeo, B. (2023). *Why make what you can mine? here's why natural hydrogen is also known as 'gold' hydrogen.* Retrieved from `https://stockhead.com.au/energy/why-make-what-you-can-mine-heres-why-natural-hydrogen-is-also-known-as-gold-hydrogen/#:~:text=Gold%20Hydrogen%20(ASX%3AGHY)&text=The%20bulk%20of%20the%20remaining,drilled%20almost%20a%20century%20ago.`

Yuan, L., Stanley, A., Dehghanpour, H., & Reed, A. (2023). Measurement of helium diffusion in lotsberg salt cores: A proxy to evaluate hydrogen diffusion. *International Journal of Hydrogen Energy*. doi: 10.1016/j.ijhydene.2023.08.003

Zahirovic, S., Matthews, K. J., Flament, N., Müller, R. D., Hill, K. C., Seton, M., & Gurnis, M. (2016). Tectonic evolution and deep mantle structure of the eastern tethys since the latest jurassic. *Earth-Science Reviews*, *162*, 293-337. doi: 10.1016/j.earscirev.2016.09.005

Zgonnik, V. (2020). The occurrence and geoscience of natural hydrogen: A comprehensive review. *Earth-Science Reviews*, *203*. doi: 10.1016/j.earscirev.2020.103140

Zhu, H., Li, X., & Xu, Y. (2020). A helium stratified and ingassed lower mantle: resolving the helium paradoxes. *Acta Geochimica*, *39*, 4-10. doi: 10.1007/s11631-019-00378-2